Heliyon 9 (2023) e16046

Contents lists available at ScienceDirect

Heliyon

journal homepage: www.cell.com/heliyon

Research article

Precipitation, submarine groundwater discharge of nitrogen, and red tides along the southwest Florida Gulf coast

Bruce E. Kurtz [a,*], James E. Landmeyer [b], James K. Culter [c]

[a] New College of Florida, 5800 Bay Shore Rd., Sarasota, FL 34243, USA
[b] U. S. Geological Survey, 4446 Pet Ln Ste 108, Lutz, FL 33559, USA
[c] Mote Marine Laboratory, 1600 Ken Thompson Pkwy, Sarasota, FL 34236, USA

A B S T R A C T

Blooms of the dinoflagellate *Karenia brevis* occur almost every year along the southwest Florida Gulf coast. Long-duration blooms with especially high concentrations of *K. brevis*, known as red tides, destroy marine life through production of neurotoxins. Current hypotheses are that red tides originate in oligotrophic waters far offshore using nitrogen (N) from upwelling bottom water or, alternatively, from blooms of *Trichodesmium*, followed by advection to nearshore waters. But the amount of N available from terrestrial sources does not appear to be adequate to maintain a nearshore red tide. To explain this discrepancy, we hypothesize that contemporary red tides are associated with release of N from offshore submarine groundwater discharge (SGD) that has accumulated in benthic sediment biomass by dissimilatory nitrate reduction to ammonium (DNRA). The release occurs when sediment labile organic carbon (LOC), used as the electron donor in DNRA, is exhausted. Detritus from the resulting destruction of marine life restores the sediment LOC to continue the cycle of red tides. The severity of individual red tides increases with increased bloom-year precipitation in the geographic region where the SGD originates, while the severity of ordinary blooms is relatively unaffected.

1. Introduction

Blooms of the dinoflagellate *Karenia brevis* (*Kb*) occur during most years along the Florida Gulf Coast, usually lasting for a few weeks or months at average concentrations up to about 10^5 cells L^{-1} (ordinary blooms) but lasting longer at concentrations of about 10^6 cells L^{-1} (red tides) in about 20% of the years. Red tides are especially prevalent along the southwest part of the Florida peninsula (boxed region on Fig. 1a, shown in greater detail by Fig. 1b) and cause serious damage to marine life and human health [1–6] through production of cyclic polyether neurotoxins known as brevetoxins [7–10].

Red tides have a deleterious effect on local marine life and coastal economies [11] and uncertainty in their origin [12,13] has led to the proliferation of multiple hypotheses. One hypothesis is that red tides originate through upwelling of bottom water rich in nitrogen (N) caused by the Florida Loop Current (Fig. 1a) periodically breaking onto the West Florida Shelf 20–75 km northwest of Tampa Bay [14–18], with the resulting bloom being subsequently advected to the shoreline where it is able to utilize nearshore nutrients [19–21]. Direct observational measurements supporting this process are limited. An alternative hypothesis involves fixation of atmospheric N by *Trichodesmium* blooms catalyzed by iron in westerly-transported Saharan dust [22–26], but this also lacks observational evidence. Both hypotheses are natural processes and are therefore consistent with the known occurrence of red tides in this area long before anthropogenic influences could have been a factor [13].

Hypotheses linking terrestrial precipitation to red tides appeared in early Florida red tide research work [27] and in subsequent observations [28], but data validating the connection were very limited. More recently, it was suggested that an exceptionally severe

* Corresponding author. 36 Tidy Island Blvd, Bradenton, FL 34210, USA.
E-mail address: kurtz36ti@gmail.com (B.E. Kurtz).

https://doi.org/10.1016/j.heliyon.2023.e16046
Received 14 October 2022; Received in revised form 5 April 2023; Accepted 3 May 2023
Available online 6 May 2023

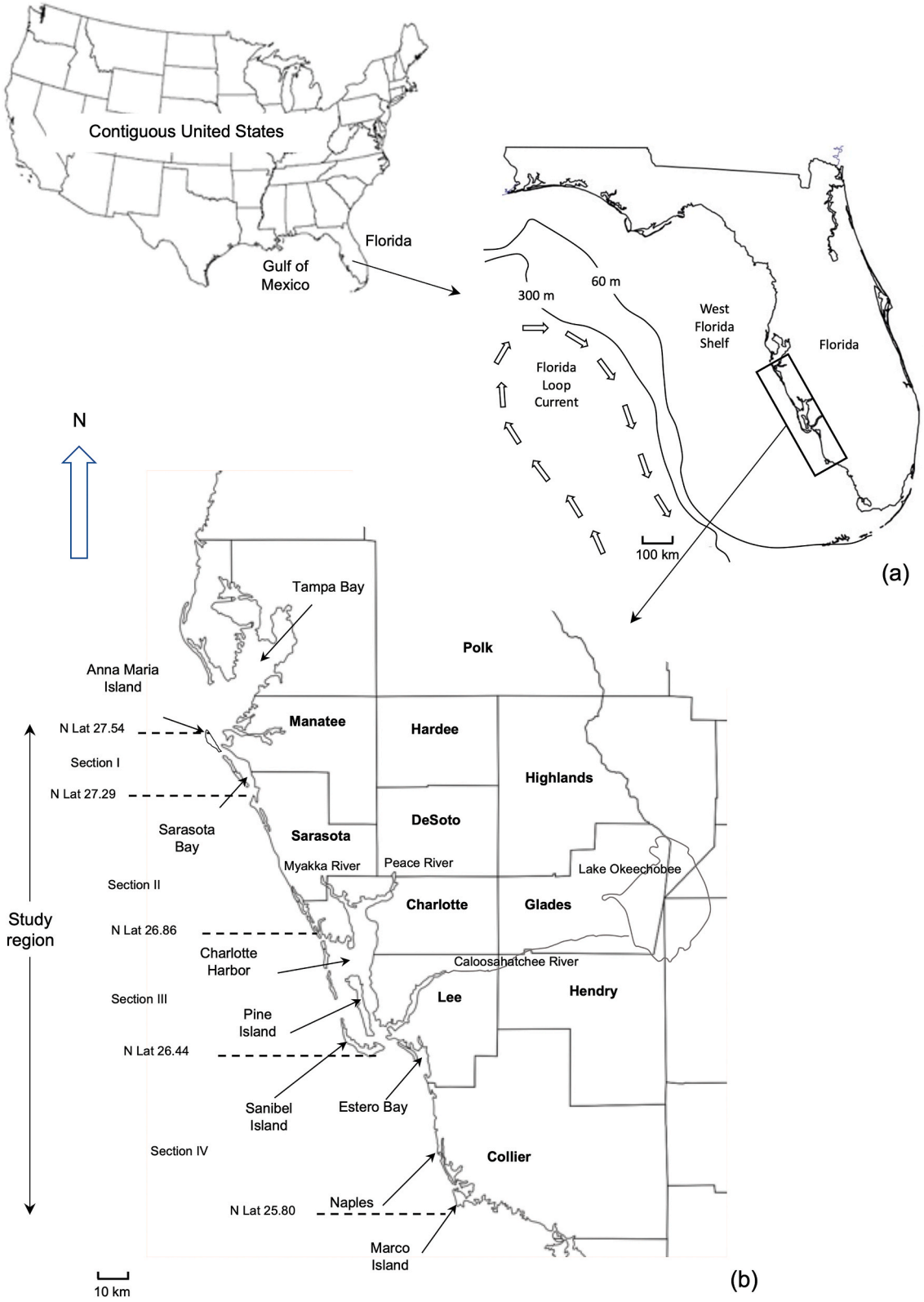

Fig. 1. (a) Florida and the West Florida Shelf. (b) Detail of the southwest part of the Florida peninsula where red tides are most prevalent (county names in bold), showing the range in latitude (Lat) of the study region and sections (see Materials and methods).

2005 red tide could have been linked to precipitation-driven submarine groundwater discharge (SGD) from a hurricane in the preceding year [29] and that SGD is a possible regular source of N for blooms [30,31]. Since terrestrial-marine nutrient flows from SGD on a regional scale often equal or exceed those from rivers, the hypothesis that SGD may be an important source of N to the West Florida Shelf is enticing [32–42]. However, a definite linkage between SGD and red tides has not been fully established.

An unanswered question about Florida red tides, perhaps more important than how they *originate*, is how they obtain the N needed to *maintain* them over a period of many months, since the N needed by a Florida red tide cannot be accounted for by known significant N sources: estuarine flux, in situ dissolved/particulate N, and decaying fish [15,20,43]. To address this "missing N" problem, we hypothesize that both the origination and maintenance of contemporary red tides can be explained by the accumulation and periodic release of terrigenous N advected via SGD to nearshore and distal bottom sediment on the West Florida Shelf.

This hypothesis involves the following sequence of naturally-occurring processes. First, (1) terrestrial precipitation recharges the shallow-to-intermediate depth coastal aquifers, (2) increasing groundwater heads and the seaward hydrologic gradient to (3) increase groundwater flow and coastward transport of nitrate (NO_3^-), which is the most common form of groundwater N [44,45]. Reducing conditions along the groundwater-flow pathways may (4) partially convert NO_3^- to nitrite (NO_2^-) and ammonium (NH_4^+), all of which

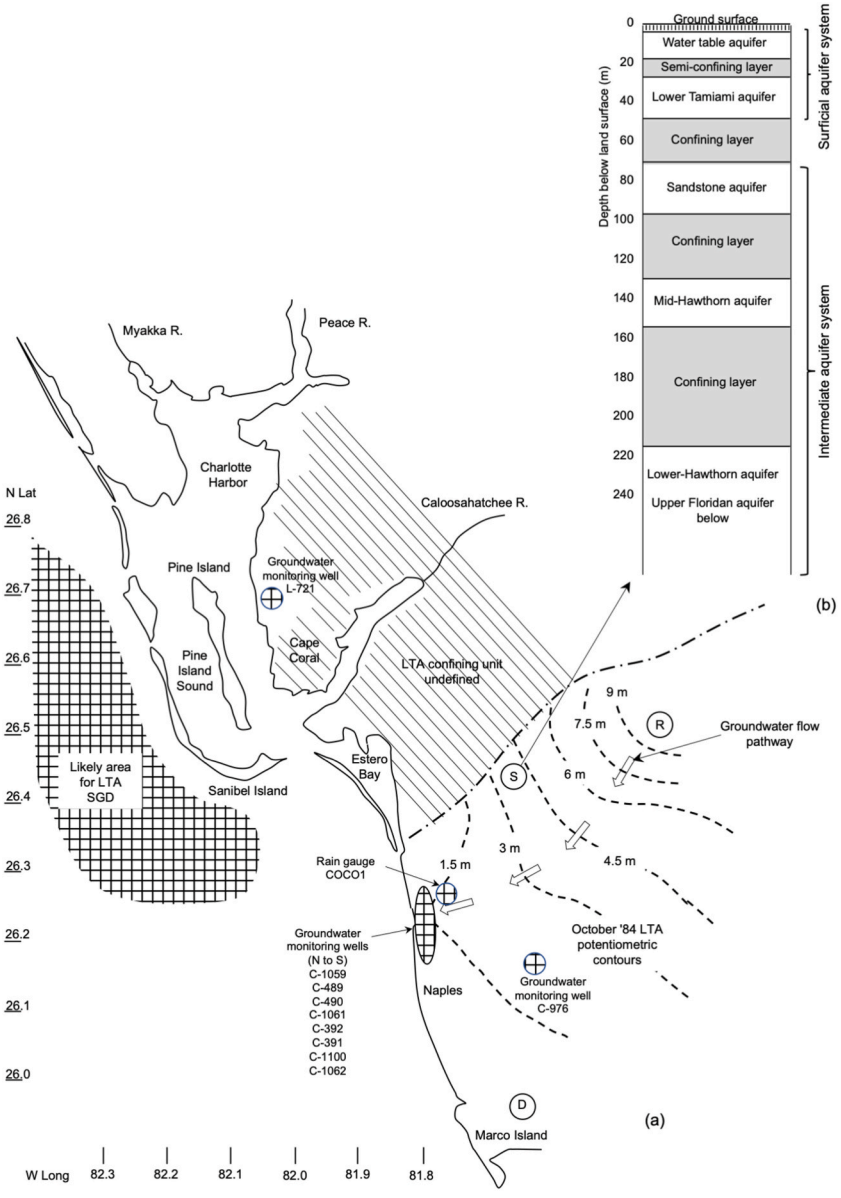

Fig. 2. (a) Detail of the part of the study region that includes the LTA. Circled letters mark terrestrial recharge (R) and discharge (D) areas. The terrestrial crosshatched areas mark monitoring well locations. The offshore crosshatched area marks an area where submarine groundwater discharge from the Lower Tamiami Aquifer is likely. (b) Approximate hydrogeological section at marked location (S).

are (5) transported by groundwater to areas of diffuse submarine seepage beneath the overlying bottom sediment, where (6) N is accumulated by dissimilatory reduction of nitrate to ammonium (DNRA) using labile organic carbon (LOC) in the sediment as the electron donor. From the sediment layer, (7) NH_4^+ and other forms of N are transported to the saltwater at the bottom of the overlying water column by upwelling of fresher SGD groundwater and are taken up by micro/macro algae and seagrass in the benthic sediment biomass. Exhaustion of the LOC, which accounts for only a small fraction of the total organic carbon in the sediment layer [46,47], eventually causes DNRA to cease, cutting off the supply of NH_4^+ to the benthic sediment biomass and causing it to die off, (8) releasing accumulated N as dissolved inorganic nitrogen (DIN) along with particulate and dissolved organic nitrogen (PON/DON), all of which are readily utilized by *Kb* [15,20], thus causing a red tide. Finally, (9) marine life detritus from the red tide restores the sediment layer LOC, thus perpetuating the cycle.

This hypothesis will be discussed in much greater detail in subsequent sections. Observational data on concentrations of *Kb* in study region waters from the Florida Fish and Wildlife Conservation Commission, precipitation data from the South Florida Water Management District, and groundwater-level data from the U.S. Geological Survey will be used to test of the hypothesis. The objective of the work presented here is to construct a firm foundation for subsequent collection of additional data needed for more conclusive testing of the hypothesis.

2. Materials and methods

2.1. Study region

The study region between Anna Maria Island and Marco Island, Florida (N lat 27.54 to 25.80), shown by Fig. 1b, is divided into four sections. The northernmost section (I) comprises Sarasota Bay and the barrier islands that separate it from the Gulf of Mexico. The section immediately to the south (II) is dominated by bays behind barrier islands, with a partial connection to the Myakka River watershed. The third section (III), comprising Charlotte Harbor and the waters around Pine Island separated from the Gulf by barrier islands, is an estuary with significant inflows of freshwater from the Myakka and Peace rivers to the north. The Caloosahatchee River, ending near the south end of Pine Island, was originally a tidal estuary but is now extensively channelized and connected to Lake Okeechobee by a canal used to release water for flood control. The tidal reach of the Caloosahatchee upstream from its mouth is about 42 km [48]. The fourth section (IV) extends from south of Sanibel Island to Marco Island, including Estero Bay and barrier islands protecting small linear bays further south. No significant freshwater streams are present in this section.

2.2. Hydrogeologic framework

The multiple aquifers underlying the study region from Charlotte Harbor (Lee County) south to Marco Island (Collier County), shown by Fig. 2a, are of special interest, with more individual aquifers in Lee County than in any other part of Florida [49]. Fig. 2b hydrogeological section at the circled location (S) on Fig. 2a shows the Surficial Aquifer System (SAS) and the Intermediate Aquifer System (IAS). Unique to this area, the SAS has two parts: the water table aquifer and the semiconfined Lower Tamiami Aquifer (LTA). The underlying IAS is itself divided into multiple parts characterized by low permeability, forming a confining unit that separates the SAS from the Upper Floridan Aquifer (UFA) further below. The SAS should be a source of nearshore (tens of meters) SGD, the LTA a source of offshore (thousands of meters) SGD, and the UFA a source of SGD to relict karst features formed under subaerial conditions during glacial maximum lower sea-level stands.

2.2.1. The surficial aquifer system in Lee and Collier counties

Both the water-table aquifer and the LTA within the SAS are recharged by precipitation, since they are separated by only a leaky, and sometimes absent, semi-confining layer [50]. The SAS/LTA exists along much of the Fig. 2a coastline, discharging close to the surface nearshore (the water-table aquifer) and also cropping out in the bottom of the Gulf of Mexico offshore (the LTA), although the exact location and nature of offshore LTA discharge is unknown. The LTA has had many names: shallow aquifer, shallow artesian aquifer, secondary artesian aquifer, and upper artesian aquifer [51], and has most recently being described as part of the Gray Limestone Aquifer extending over most of central south Florida, including eastern and central Collier County and southern Hendry County [52].

North of Lee County the SAS consists of only a water-table aquifer [49,53–55], which directly overlies the IAS. The IAS, which is recharged in Polk County, is an unlikely source of SGD since it has a much lower transmissivity than the LTA [56–58]. By contrast, the SAS in Sarasota, DeSoto, and Charlotte counties is an obvious path for conveying groundwater to the Gulf via shoreline SGD and to Charlotte Harbor via the Peace and Myakka stream valleys [59,60].

2.2.2. The water-table aquifer part of the SAS

An idealized flow-net representation of water-table aquifer groundwater flow through a homogeneous permeable bed to the sea indicates that freshwater will escape through a gap between the shoreline and the body of saltwater [61]. The width of the gap is:

$$x_0 = \frac{Q}{2\gamma K} \tag{1}$$

where: Q = freshwater volumetric flow per unit length of shoreline, γ = fractional difference between the density of saltwater and

freshwater, K = hydraulic conductivity of the strata through which freshwater is discharged.

The value of Q can be estimated from the rate of decrease in groundwater level following a precipitation event, obtained from monitoring wells close to the shoreline.

In contrast to this idealized representation, freshwater discharge from a water-table aquifer actually occurs in a diffuse transition zone that is constantly moving due to tidal pumping, wave action, aquifer anisotropy, and concentration gradients. A dynamic wedge of saltwater intrudes under the freshwater, moving inland with low aquifer flow and seaward with high flow. Kinetic energy supplied from wave and tidal actions increases dispersion of salt into the freshwater, causing saltwater to recirculate through the mixing zone [62,63]. What appears to be an unconfined, homogeneous water-table aquifer may actually behave like a layered aquifer with freshwater discharging beneath seawater at several levels because of thin silt layers within the aquifer [64].

Such systems, described as subterranean estuaries [36,65], support biogeochemical reactions that alter the oxidation state of terrigenous N transported by groundwater [66], just as with surface estuaries. The solid matrix of the sediment reduces diffusion and advection, creating redox gradients where concentrations of N in various oxidation states are much higher than in the overlying water column and anoxia causes a shift toward more reduced N forms [67]. With NH_4^+ released from the sediment layer, local phytoplankton community composition will tend to shift from diatoms towards dinoflagellates [68–72].

2.2.3. The LTA part of the SAS

The LTA probably ends south of the peninsula forming the west side of Charlotte Harbor and north of monitoring well L-721 [73,74]. The LTA confining unit is undefined in the hatched area of Fig. 2a but reappears on Pine Island and on the barrier islands to the south and west [75]. The LTA on Sanibel Island lies below the water-table aquifer at a depth of about 10 m [53,76], which is the basis for estimating the likely area for offshore LTA SGD on Fig. 2a. A semi-confined artesian aquifer, like the LTA, can discharge at a much greater distance from shore than a water-table aquifer [33].

The LTA, composed of solution-riddled limestone [77], has a potentiometric surface consistently higher than the water-table [78], both of which are higher than mean sea level. The LTA potentiometric contours for October '84 on Fig. 2a show a potential height relative to mean sea level of 1.5 m close to the coastline north of Naples, while in April of the same year the potential height at that location was at or below zero, consistent with seasonal highs and lows in precipitation [54,79]. Recharge to the LTA occurs over most of the area shown by the potentiometric contours, including at the potentiometric high (R) where the LTA confining layer is absent and aquifer transmissivities are very high [80]. By contrast, terrestrial locations of LTA discharge (D) are limited to a much smaller area north of Marco Island and account for less than 22% of the mapped aquifer area [81]. Most of the discharge from the LTA occurs by SGD to the Gulf of Mexico, along with vertical leakage, and withdrawal from wells [54,80].

2.2.4. Precipitation and tidal forcing

Precipitation is the dominant driver of SGD during times when groundwater levels are high relative to the range of tide. When this is not the case, wave and tidal actions strongly influence rates of SGD [82], which will be much lower than during times of high groundwater level. In confined or semi-confined aquifers, SGD response to tides is driven by tidal loading, which is the weight of seawater exerting a downward force on the aquifer matrix, rather than by hydraulic connection [64]. Tidal loading on the "shallow artesian aquifer" (LTA) causes fluctuations of levels in monitoring wells on Sanibel Island [53] and an LTA tidal signal comprising two small daily peaks is detected more than 40 km east of the monitoring wells [52].

2.3. Anthropogenic N and groundwater

The production of synthetic N fertilizer worldwide increased about 20-fold over the last 50 years [83], roughly doubling the rate of N input to the terrestrial N cycle and greatly altering the composition and functioning of estuarine and nearshore ecosystems [84]. The consumption of synthetic N fertilizer per unit area of cropland in the United States increased by a factor of about four between 1960 and 1990 but has increased at a much slower rate since then [85]. Nitrate concentrations in Florida's Peace River, which flows into Charlotte Harbor, followed this pattern, increasing by more than 10-fold between 1960 and 1980 but only slightly since then [86].

In general, 50–70% of N applied to the soil is lost to groundwater by leaching [87], depending on soil type. The soils in the study region, predominantly spodosols, are especially prone to leaching of N [88]. This source of N in the environment is much larger than all other anthropogenic sources combined, perhaps as much as 95% of the total [89].

Poorly drained soils, low dissolved oxygen concentrations, and high organic carbon content encourage reduction of NO_3^- to NO_2^- and NH_4^+, or to N_2 via denitrification [90–92]. As a result, streams and groundwater in the Southeast U.S. generally contain relatively low concentrations of NO_3^-. By contrast, well-drained and well-oxygenated soils in the California Central Valley, parts of the Northwest, Northern Plains, and Mid-Atlantic regions favor NO_3^- persistence and transport into groundwater. Because of their high permeability, unconsolidated sand and gravel aquifers of the kind found in the study region have high concentrations of NO_3^-, whether under agricultural or urban conditions [45].

Depending on soil conditions, N can persist in groundwater as NO_3^- for decades [45,93–95]. Even with complete cessation of fertilizer application, this "legacy nitrogen" will prevent any immediate decrease in groundwater N concentration. As an example, modeling predicts a biogeochemical lag time of 35 years for soil organic nitrogen in the Mississippi River Basin [96,97].

2.4. Data sources

Data on study region hydrogeology, groundwater, precipitation, and *Kb* concentrations were gathered from multiple sources, as

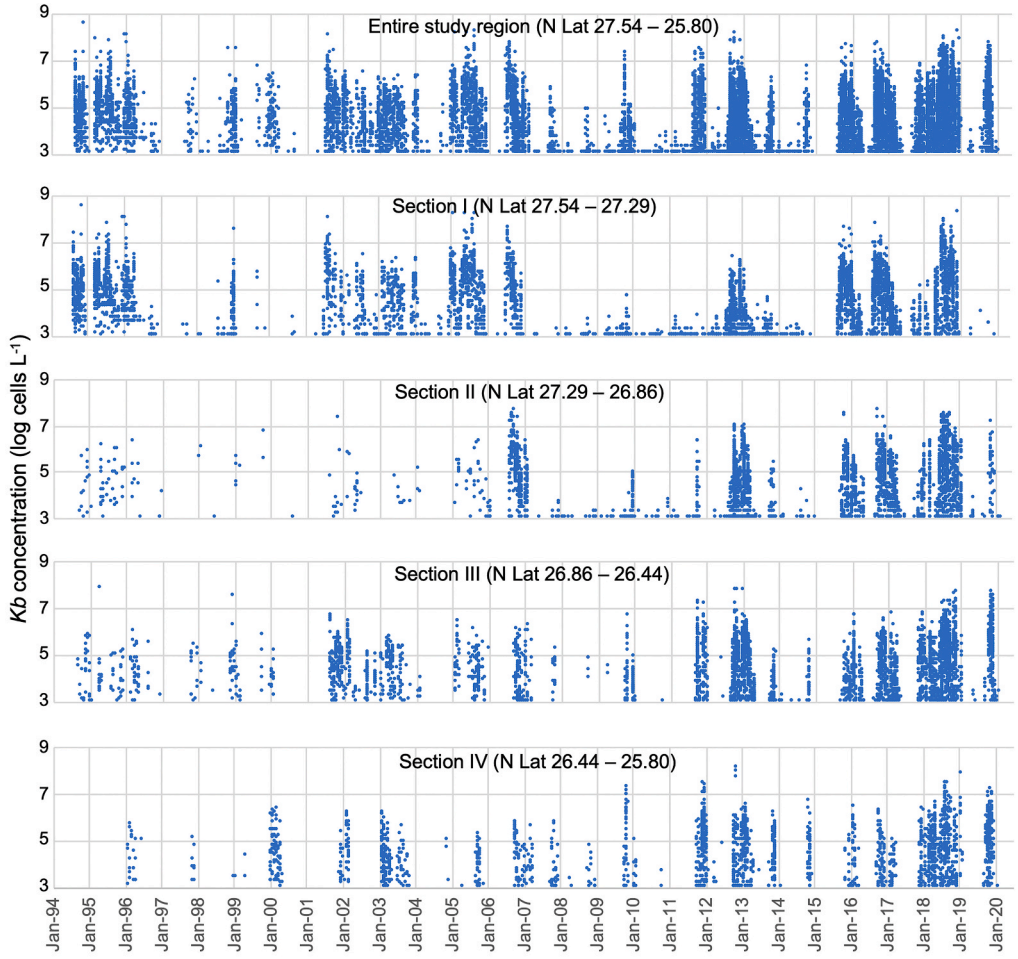

(a)

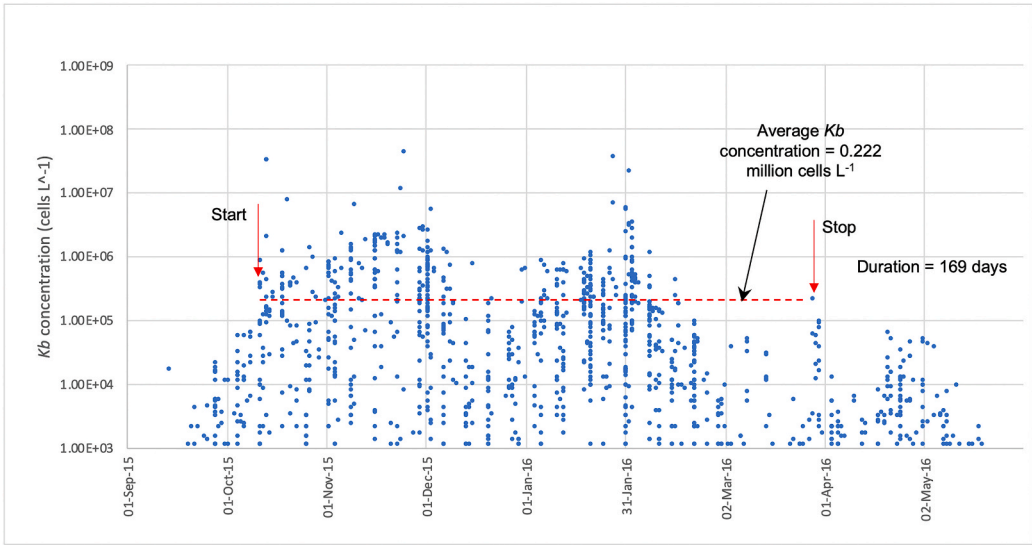

(b)

Fig. 3. (a) Time series of *Karenia brevis* (*Kb*) concentrations for the entire study region, north latitude (N Lat) 27.54–25.80, and individual region sections from 1994 to 2020. (b) Example bloom severity calculation using the 2015 bloom time series of *Karenia brevis* concentrations. Bloom severity is the product of bloom average *Kb* concentration in million cells L^{-1} and bloom duration in days, in this case $0.222 \times 169 = 38$.

described below.

2.4.1. Groundwater levels and precipitation amounts

Groundwater level data in monitoring wells came from the U.S. Geological Survey - National Water Information System [98]. Precipitation amount data near the large group of monitoring wells on Fig. 2a came from the South Florida Water Management District (SFWMD) COCO1 precipitation gauge located close to well C-1059 at north latitude 26.273, west longitude 81.780 [99]. Levels in the C-1059 monitoring well were recorded on a more-or-less monthly basis but not on any particular date, while precipitation was recorded on a daily basis, so we normalized precipitation to groundwater levels by adding together daily precipitation amounts to obtain cumulative precipitation between level readings. Precipitation amounts for individual counties having the potential to supply groundwater to the coastal part of the study region came from the National Oceanic and Atmospheric Administration – National Centers for Environmental Information website [100].

2.4.2. Karenia brevis concentrations

We obtained data on *Kb* concentrations from the Florida Fish and Wildlife Conservation Commission, Fish and Wildlife Research Institute (FWC-FWRI) Harmful Algae Bloom Monitoring Database (habdata@MyFWC.com). Sampling prior to 1994 was discontinuous, generally not starting until a bloom was well-established [101]. Nearly continuous sampling began with the severe 1994–95 red tides but was mostly limited to section I of the study region, with frequency decreasing over the following years until another red tide in '01. Sampling frequency and spatial scope were increased after severe red tides in 2005–2006.

Because *Kb* blooms are heterogeneous, time series of sample concentrations appear as a cloud of data points, shown by Fig. 3a, with zero *Kb* concentrations found even during red tides when the average *Kb* concentration is around 10^6 cells L^{-1}. Concentrations are shown for both the entire study region (top) and its four sections. The low density of data points from sections II–IV during the earlier years reflects low rates of sampling. Details are in Supplemental Data File S1 – Sampling.

2.5. Calculation of bloom severity and regression against precipitation

Determining the effects of external variables on the severity of *Kb* blooms requires a *quantitative* definition of severity, so we define bloom severity (S_B) as the product of bloom average *Kb* concentration (C_{avg}) in millions of cells L^{-1}, and bloom duration (D) in number of days from first to last *Kb* concentration $\geq 1 \times 10^5$ cells L^{-1}, the approximate concentration at which fish mortality begins [102].

$$S_B = C_{avg} D \tag{2}$$

The heterogeneous nature of *Kb* blooms requires that bloom average *Kb* concentration be based on *all* measurements, including those detecting no *Kb*. The calculation method is illustrated by Fig. 3b. Details are in Supplemental Data File S2 – Time series.

Table 1
Monitoring well data from U.S. Geological Survey (USGS): Well name and station identification (ID), location north latitude (N Lat), north longitude, (N Long), distance to shore, total depth below land surface (BLS), land surface elevation, average (Avg) peak groundwater (GW) levels above mean sea level (AMSL) and BLS. Depths in m, distance to shore in km. Average peak GW levels were calculated as the average of peak annual values for 1990–2020 (standard deviations in parentheses). Depths to the freshwater/saltwater interface (FW/SW) were calculated from the Ghyben-Herzberg relation.

Well name and USGS station ID	N Lat	N Long	Distance to shore	Total depth BLS	Land surface elevation	Avg peak GW level AMSL	Avg peak GW level BLS	Depth to FW/SW interface
L-721 261302081473901	26.698	82.039	2.4	5.5	1.0	1.0 (0.19)	0.0	41
C-1059 261604081480901	26.268	81.803	2.5	7.6	2.4	2.0 (0.23)	0.4	80
C-489 261302081473901	26.224	81.792	2.6	25.3	4.2	1.4 (0.51)	2.8	56
C-490 261243081480301	26.221	81.800	1.9	21.6	4.7	1.6 (0.32	3.1	65
C-1061 261311081480101	26.220	81.800	1.9	7.6	4.2	3.8 (0.17)	0.4	152
C-392 261124081470101	26.190	81.791	2.4	9.1	2.7	2.1 (0.17)	0.6	84
C-391 261124081470301	26.190	81.792	2.4	22.9	2.6	1.3 (0.38)	1.3	51
C-1100 261023081463702	26.173	81.777	3.7	4.9	1.7	0.5 (0.11)	1.2	21
C-1062 260925081475101	26.158	81.798	1.9	7.3	2.9	2.2 (0.15)	0.7	89
C-976 260915081385901	26.154	81.646	16.3	12.2	3.2	2.5 (0.29)	0.7	99

We determined coefficients (R-squared) and two-tailed p-values for regression of the calculated bloom severity against annual precipitation in individual counties likely to contribute to groundwater flows to the coastline of the study region. Values of R-squared represent the fraction of the variation in bloom severity explained by the variation in annual precipitation. Two-tailed p-values represent the probability that the null hypothesis cannot be rejected.

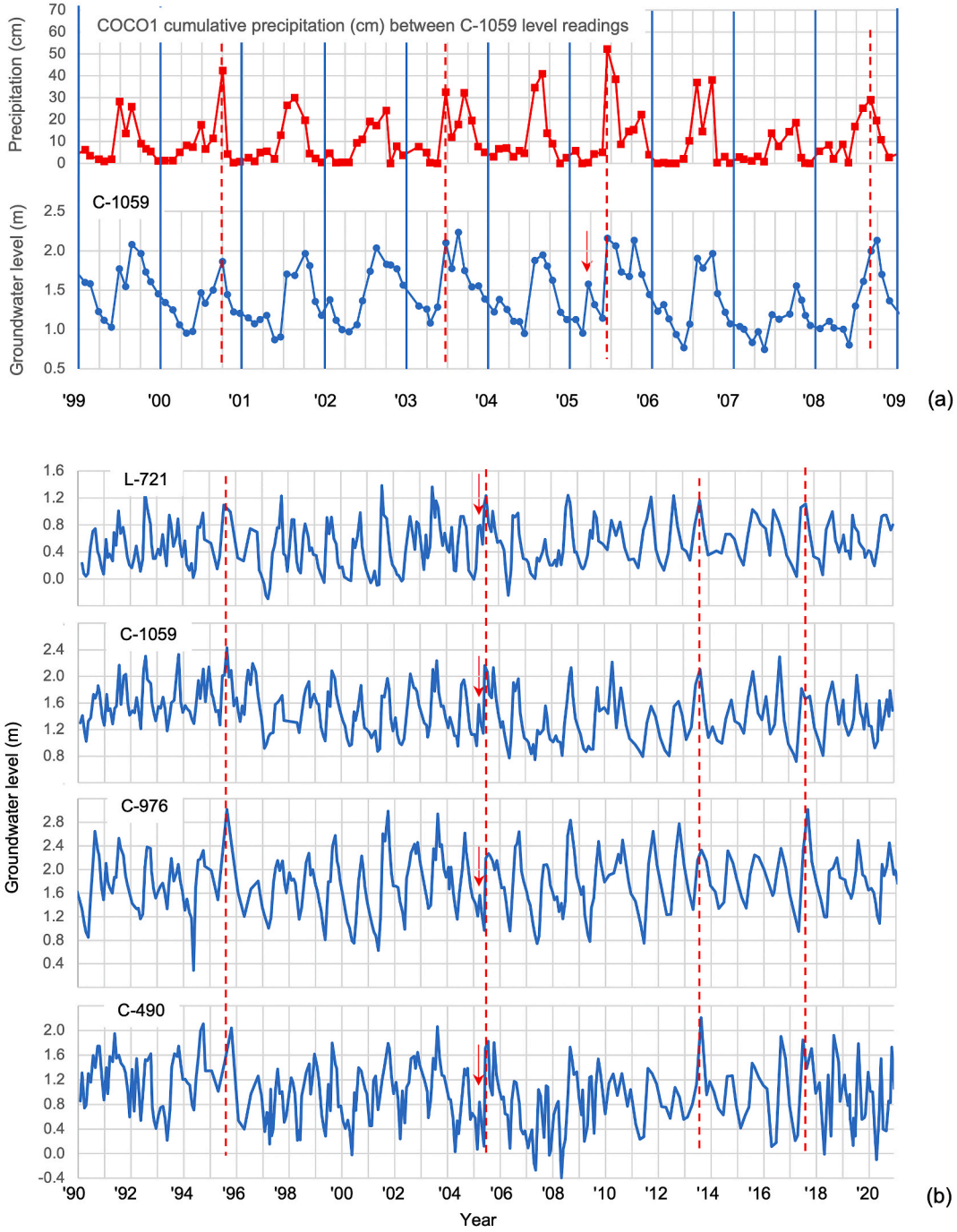

Fig. 4. (a) COCO1 normalized precipitation and groundwater (GW) levels in well C-1059 for 1999 through 2009 (blue lines mark end-of-year, dashed red lines illustrate synchronization between precipitation events and groundwater levels). (b) Comparison of GW levels between different monitoring wells for 1990 through 2020 (dashed red lines illustrate synchronization between groundwater levels in different wells). Levels are above mean sea level. Red arrows mark a precipitation event in Lee County not detected by the COCO1 precipitation gauge. (For interpretation of the references to colour in this figure legend, the reader is referred to the Web version of this article.)

3. Results and discussion

3.1. SGD drivers and flow rates

As we stated before, SGD is driven by a seaward groundwater gradient (difference in groundwater levels) that depends on net recharge (a function of precipitation, infiltration, and evapotranspiration), as well as on tidal forcing.

3.1.1. Groundwater levels

Table 1 shows USGS information on the groundwater level monitoring wells used in this study (Fig. 2a). We calculated "average peak groundwater levels" as the arithmetic averages of the annual peak values over 1990–2020, with depths to the freshwater/saltwater interface calculated by the Ghyben-Herzberg relation [103,104]. That depth is significant because it supports seaward flow of SGD from confined and semiconfined aquifers that is not countered by tidal effects, in contrast to the periodic landward flow of saltwater in surface estuaries, rivers and streams. An important observation related to the nearly co-located C-392 (in the water-table part of the SAS) and C-391 (probably in the LTA) is the downward vertical head gradient, consistent with the mapping of LTA recharge areas [81], which demonstrates a potential for recharge very close to the shoreline and a likely rapid response by SGD to precipitation.

Fig. 4a compares the cumulative precipitation collected by the COCO1 gauge between level readings for well C-1059 during 1999–2009, a time when levels were measured more frequently than usual. The degree of synchrony between the two variables is remarkable (dashed red lines show examples). Groundwater level increases quickly in response to precipitation events, consistent with rapid infiltration through the empty pore spaces above the water-table. Outflow, seen as a decrease in level, is evident immediately following cessation of precipitation, consistent with high aquifer transmissivity. These results are similar to those obtained from a study in the western Mediterranean Sea, where SGD increased by an order of magnitude following an extreme precipitation event [105]. Groundwater levels generally peak in August–September (sooner if there is a major precipitation event), then decline to a minimum during April–May of the following year.

The average annual decrease in groundwater level from peak accumulation, presumably representing SGD, is 108 cm for C-1059. With an assumed water-table aquifer specific yield of 0.15 (one-half of a likely aquifer porosity of 0.30), this is equivalent to 16 cm of captured precipitation, accounting for 13% of the 123 cm average annual COCO1 amount of precipitation. Additional SGD will occur during the time when groundwater is being accumulated. The remainder of the precipitation will be largely lost to evapotranspiration, with little or none lost as surface runoff [106].

Fig. 4b compares groundwater levels in L-721, C-1059, C-490 and C-976 over a longer time period (1990–2020). Wells L-721, C-1059, and C-976 are in the water table part of the SAS, while C-490 is in the LTA. Changes in level are well-synchronized, even for well C-490 in the LTA. Well C-976, which is located about 16 km inland, has the highest amplitude, as would be expected.

A change in level with no corresponding COCO1 precipitation event, marked by the red arrow on Fig. 4a C-1059 (near 1-Apr-05), was caused by a 17-cm Lee County precipitation event [100] that was visible in well L-721 (Fig. 4b) in that county, but also visible in wells C-1059, C-976, and C-490 (red arrows) in Collier county, more than 50 km south, even though the precipitation event did not extend far enough to be captured by the COCO1 gauge.

3.1.2. Estimated nearshore SGD flow rate and freshwater gap

The rate of SGD following peak groundwater level was estimated from the rate of groundwater level decrease, about 0.02 m d^{-1} based on well C-1059 (the other monitoring-well groundwater levels drop at similar rates). With aquifer specific yield of 0.15 and assuming that the change in groundwater level extends inland for 5 km, the volumetric flow per meter of shoreline (Q) was 15 m^3 d^{-1} per meter of shoreline (1.7×10^{-4} m^2 s^{-1}). This compares to values ranging from 0.5 to 6 m^3 d^{-1} per meter of shoreline for Tampa Bay, calculated using various methodologies [34]. The annual amount of SGD (water table plus LTA) from the area represented by the monitoring wells based solely on the seasonal decrease in groundwater level of about 1 m and the above aquifer specific yield is 750 m^3 m^{-1} of shoreline.

For water-table aquifer discharge with the above Q value, $\gamma = 0.025$, and $K = 1.5 \times 10^{-4}$ m s^{-1} (coarse sand), eq. (1) predicts a freshwater gap (x_0) of 23 m. Martin et al. (2007) obtained a similar result with a much lower value for Q and a proportionally lower value for K [35]. While of only qualitative accuracy, this result indicates that SGD from the water-table aquifer does not extend very far from shore.

3.2. Benthic N accumulation and release to the Gulf of Mexico

According to our hypothesis, benthic N accumulation and release to the Gulf of Mexico involves delivery of groundwater N to benthic sediment via SGD, accumulation in benthic sediment biomass via DNRA, and subsequent N release due to exhaustion of sediment LOC. The data for these interconnected processes are shown in separate subsections below.

3.2.1. Groundwater N

Based on data from the Collier County Watershed Management plan [107], concentrations of total N derived from wells in the vicinity of the groundwater level monitoring wells (C-1059 and southward) are in the range of 1.6 mg L^{-1} (screening criterion for N in streams) to 10 mg L^{-1}. Some of these N monitoring wells are associated with the County's water reuse program, where N concentrations are about 10 mg L^{-1}, but water quality analyses indicated no significant difference in total N among the wells except for a few locations with known issues [108]. Nitrogen concentrations are >10 mg L^{-1} immediately to the east of the groundwater level

monitoring wells.

The land in the vicinity of the monitoring wells near the shoreline appears to have been developed from freshwater marshes, where N concentrations might be expected to be lower than for the agricultural lands further inland. On the other hand, legacy N beneath the agricultural lands will have migrated toward the shoreline over the many decades when there were heavy applications of synthetic N fertilizer. A typical N concentration in groundwater beneath agricultural land is 3 mg L^{-1} (210 μM), [45,109]. Using this value and an annual SGD flow of 750 m^3 m^{-1} of shoreline (Section 3.1.2), the annual SGD-N will be 160 mols per meter of shoreline. For comparison, annual SGD-N from a region along the coast of the southeastern Mediterranean with similar concentrations of N in groundwater was reported to be about 500 mols per meter of shoreline [110].

3.2.2. *The DNRA part of the hypothesis*

Since known sources of nearshore N are not sufficient to realistically support a red tide, a possible means by which the missing N could be supplied is benthic accumulation of SGD-N during years when no red tides occur, followed by release of that N due to the collapse of the accumulation process, as shown by Fig. 5.

When DNRA is active, NO_3^- advected by SGD (nearshore or offshore) into the anoxic sediment will either be converted to NH_4^+ by DNRA or undergo canonical denitrification to N_2. If the former, the NH_4^+ will be assimilated into the benthic sediment biomass with little or no NO_3^- escaping into the water column. The DNRA reaction depends on the availability of LOC as the electron donor and will cease when the LOC is exhausted [111]. When deprived of NH_4^+, the benthic sediment biomass will die and release N as DIN, PON, and DON. The detritus from the resulting red tide will restore the LOC content of the sediment layer to continue the cycle of red tides.

An important condition for *Kb* bloom formation is that the normal N concentration in the region subject to periodic release of N from the benthic biomass be too low to support faster-growing algae found in N-rich nearshore waters, thus allowing rapid growth of the region's *Kb* population in response to the sudden release of benthic N. Concentrations of N in the Gulf beyond the West Florida Shelf are typically <0.1 μM [112] and these conditions may persist as close as 1–2 km from shore [113,114].

A nascent red tide in this region, adjacent to N-rich nearshore waters dominated by the faster-growing algae, could quickly intrude into those waters if aided by *Kb* allelochemicals. These are sublethal and slow-acting compared to those of other allelopathic algae, but

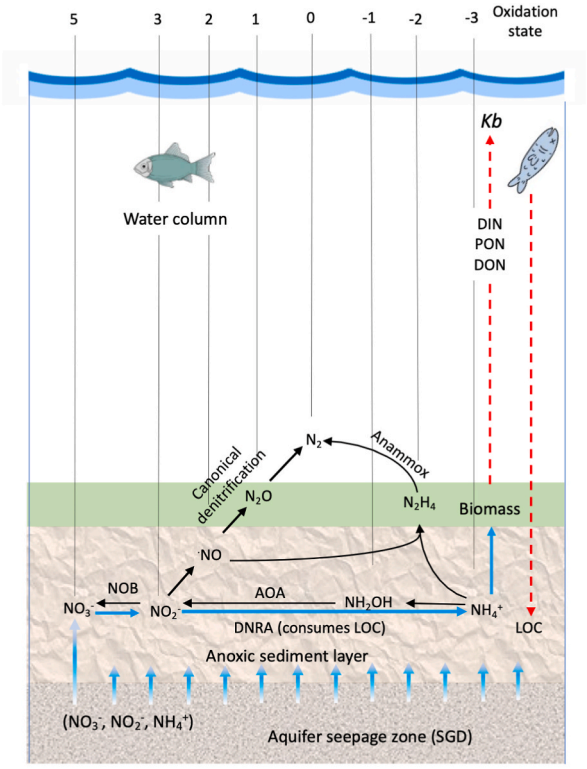

Fig. 5. Hypothesized DNRA process for benthic accumulation and release of N to support a red tide, showing seepage of submarine groundwater into benthic sediment and subsequent reactions. Blue arrows represent accumulation of N, dashed red arrows represent release, black arrows represent possible competing reactions. (For interpretation of the references to colour in this figure legend, the reader is referred to the Web version of this article.)

they weaken cell membranes, reduce photosynthesis, and impair osmoregulation in competing algae [115–120]. Once established nearshore, *Kb* could then become dominant by exploiting vertical migration, selective shading, and mixotrophy [121–126].

This mechanism does not explain the rapid propagation of a red tide into areas that are not subject to offshore SGD-N along the coastline and bays behind the barrier islands. It is possible that N will have accumulated in these areas by DNRA of nearshore, diffuse SGD-N, and perhaps by direct uptake from the water column, so it is interesting to speculate whether this N is made available to an advancing red tide by *Kb* allelochemical inhibition of the single enzyme mediating conversion of NO_2^- to NH_4^+ in DNRA, cytochrome *c* nitrite reductase [127].

3.2.3. *Reactions that compete with DNRA*

Canonical denitrification competes with DNRA for the same NO_3^-, with the Gibbs free energy change favoring the latter. But energy losses from multiple enzymatic reaction steps in denitrification favor DNRA, especially when NO_3^- is limited relative to sediment LOC [128–130]. The nature of the particulate LOC also affects this competition [131]. DNRA is favored over denitrification by conditions often found in coastal regions: high LOC loads, high C/N ratio organic matter, low NO_3^- concentrations, and high rates of SO_4^{2-} reduction [132–135]. High sulfide concentrations enhance DNRA by competitive exclusion, providing more electron donors to inhibit competition from nitrification and denitrification [136]. High water temperatures [137] also favor DNRA: it is dominant over denitrification in estuarine sediments during the summer months [138]. Seagrass communities, which are extensive in the shallow coastal and estuarine waters of the study region, favor DNRA over denitrification because seagrass detritus has a higher C/N ratio than phytoplankton detritus [132,139,140].

In addition to losses due to denitrification, N can be lost by anammox (anaerobic ammonium oxidation), where nitrogen gas (N_2) is formed via the simultaneous availability of NO_2^- and NH_4^+, a condition found only at the aerobic-anaerobic sediment interface. Since NO_2^- concentrations are low in the presence of excess NH_4^+ and LOC, anammox should be unimportant in the hypothesized system [141,142].

Nitrification reverses the effect of DNRA by converting NH_4^+ back to NO_3^-. It is an aerobic process occurring either in two steps with ammonium-oxidizing archaea (AOA) producing NO_2^- via hydroxylamine and nitrite-oxidizing bacteria (NOB) producing NO_3^- [143,144], or in a single step by way of comammox bacteria [145]. Since anoxic conditions exist in all but the top few mm of sediment layers in coastal areas [146], nitrification should be unimportant.

3.2.4. *N storage in the benthic sediment biomass*

The benthic microalgae (BMA) in the upper few centimeters of the sediment layer have a much larger biomass than that of the water column above [147,148] and are potentially a major reservoir for SGD-N. It has been suggested that SGD is the main source of "new" N for BMA in the South Atlantic Bight [149], so it is reasonable to expect this to be true for that part of the study region in Florida that is susceptible to SGD. BMA can prolong phytoplankton blooms by storing NH_4^+ during winter/spring and releasing it in the summer when growth becomes light-limited through phytoplankton shading [67], so it is possible that this also occurs with red tides limited by *Kb*

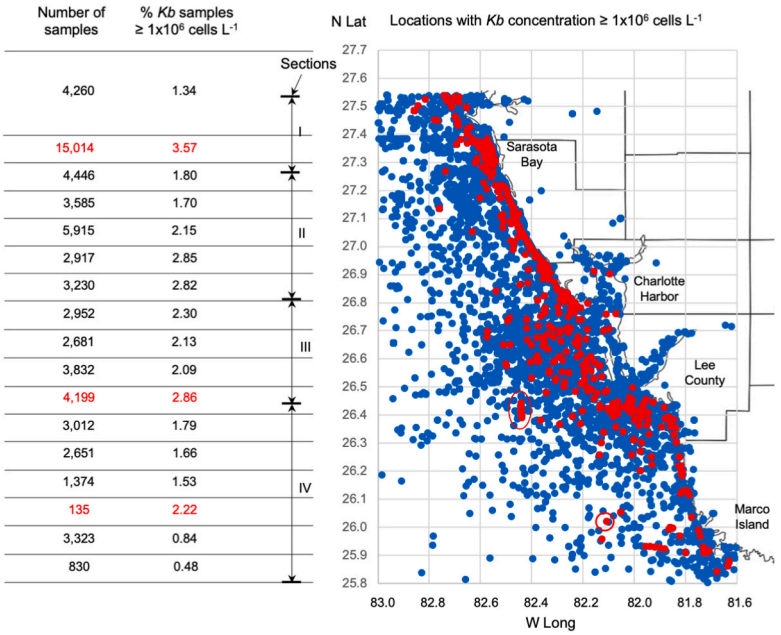

Fig. 6. Sample locations (blue) and locations with *Kb* concentration $\geq 1 \times 10^6$ cells L^{-1} (red) for the 1994–2020 study period; circles mark hotspots that suggest possible karst SGD-N features; table shows number of samples and % samples $\geq 1 \times 10^6$ cells L^{-1} for each latitude (lat) band; results in red are local maxima. (For interpretation of the references to colour in this figure legend, the reader is referred to the Web version of this article.)

self-shading. The amount of stored intracellular NO_3^- in bottom sediment can be much greater than that in porewater because, while DNRA is most common in prokaryotes, some eukaryotes employ autotrophic DNRA and store NO_3^- intracellularly [134,150,151].

Ammonium is taken up by the benthic biomass more readily than NO_3^- because it can be assimilated in its present oxidation state. For example, in an Australian seagrass community, the uptake of NO_3^- was only about one-sixth that of NH_4^+ [140]. In addition to assimilating NH_4^+ produced by DNRA, NO_3^- and NH_4^+ can be taken up directly from the water column by BMA, macroalgae, and seagrass [132,152,153]. Direct uptake is especially likely in shallow nearshore and estuarine locations subject to surface water nutrient flows from the mainland.

3.2.5. *Offshore locations with high Kb concentration*

Fig. 6 shows the locations of samples with concentrations of *Kb* $\geq 10^6$ cells L^{-1}. The lat 26.3–26.7 area with many high-*Kb* concentration offshore sample locations coincides with the likely area for LTA SGD shown by Fig. 2a. To control for the number of samples, the table part of the figure shows the percentage of samples with *Kb* concentrations $\geq 1 \times 10^6$ cells L^{-1} in 0.1-degree latitude segments. The N Lat 27.3–27.4 segment is biased by the large number of samples taken during red tides in the Sarasota County part of Sarasota Bay and can be disregarded. The 26.4–26.5 segment shows a large percentage of high-concentration *Kb* samples from multiple locations immediately south of Sanibel Island and at an offshore "hotspot" (circled) with an average *Kb* concentration of 5.9×10^6 cells L^{-1} (November 2009). The N Lat 26.0–26.1 segment result reflects a single offshore sample with an average *Kb* concentration of 7.7×10^7 cells L^{-1} (November 2011). These offshore hotspots may represent SGD-N from karst features and are worthy of further investigation.

3.3. *Testing the hypothesis*

We will show how the DNRA hypothesis predicts that the severities of ordinary blooms and red tides will respond differently to changes in bloom-year precipitation, then we will use calculated bloom severities and precipitation data to test this prediction.

Table 2
Calculated *Karenia brevis* (*Kb*) bloom severities and related information from the 1994–2020 study period plus additional results from 1984 to 1993 (in italics). Red tides shown in red. Details are in the Supplemental Data File (S3 – Regression).

Year	Start date	Start day-of-year	Duration (days)	Max Kb conc (cells L^{-1})	Avg Kb conc (cells L^{-1})	Severity (S_B)
1984	*26-Jan-84*	*26*	*151*	*1.17E+06*	*1.15E+05*	*15*
1985	*23-Oct-85*	*296*	*7*	*1.13E+06*	*2.15E+05*	*2*
1986	*16-Sep-86*	*259*	*73*	*3.71E+06*	*1.75E+05*	*13*
1987	*3-Feb-87*	*34*	*122*	*1.41E+06*	*9.53E+04*	*12*
1988	*No bloom*	*No bloom*	—	—	—	*0*
1989	*No bloom*	*No bloom*	—	—	—	*0*
1990	*No bloom*	*No bloom*	—	—	—	*0*
1991	*29-Jul-91*	*210*	*59*	*2.73E+07*	*5.23E+05*	*31*
1992	*3-Sep-92*	*247*	*90*	*1.15E+08*	*1.84E+06*	*165*
1993	*No bloom*	*No bloom*	—	—	—	*0*
1994	19-Sep-94	262	121	3.58E+08	1.36E+06	164
1995	13-Apr-95	103	424	1.19E+08	7.12E+05	302
1996	No bloom	No bloom	—	—	—	0
1997	23-Oct-97	296	81	1.31E+06	2.00E+04	2
1998	1-Dec-98	335	84	3.44E+07	3.95E+05	33
1999	1-Oct-99	274	202	5.91E+06	1.46E+05	30
2000	No bloom	No bloom	—	—	—	0
2001	21-Aug-01	233	240	1.15E+08	6.65E+05	160
2002	1-Jul-02	182	64	2.88E+06	8.00E+04	5
2003	23-Jan-03	23	263	2.12E+06	5.47E+04	14
2004	15-Jan-04	15	39	2.11E+06	1.05E+05	4
2005	26-Jan-05	26	351	1.62E+08	7.78E+05	273
2006	31-Jul-06	212	226	5.56E+07	4.98E+05	113
2007	No bloom	No bloom	—	—	—	0
2008	No bloom	No bloom	—	—	—	0
2009	24-Oct-09	297	75	2.11E+07	1.24E+05	9
2010	No bloom	No bloom	—	—	—	0
2011	26-Sep-11	269	108	3.14E+07	2.46E+05	27
2012	1-Oct-12	275	169	1.51E+08	3.77E+05	64
2013	28-Oct-13	301	29	1.82E+06	2.49E+04	1
2014	23-Oct-14	296	32	5.55E+06	3.12E+04	1
2015	12-Oct-15	285	169	4.19E+07	2.22E+05	38
2016	19-Sep-16	263	198	6.14E+07	2.55E+05	50
2017	13-Nov-17	317	184	6.48E+06	5.16E+04	9
2018	4-Jun-18	155	196	9.11E+07	9.78E+05	192
2019	30-Sep-19	273	71	5.37E+07	7.37E+05	52
2020	1-Dec-20	336	226	1.15E+07	1.28E+05	29

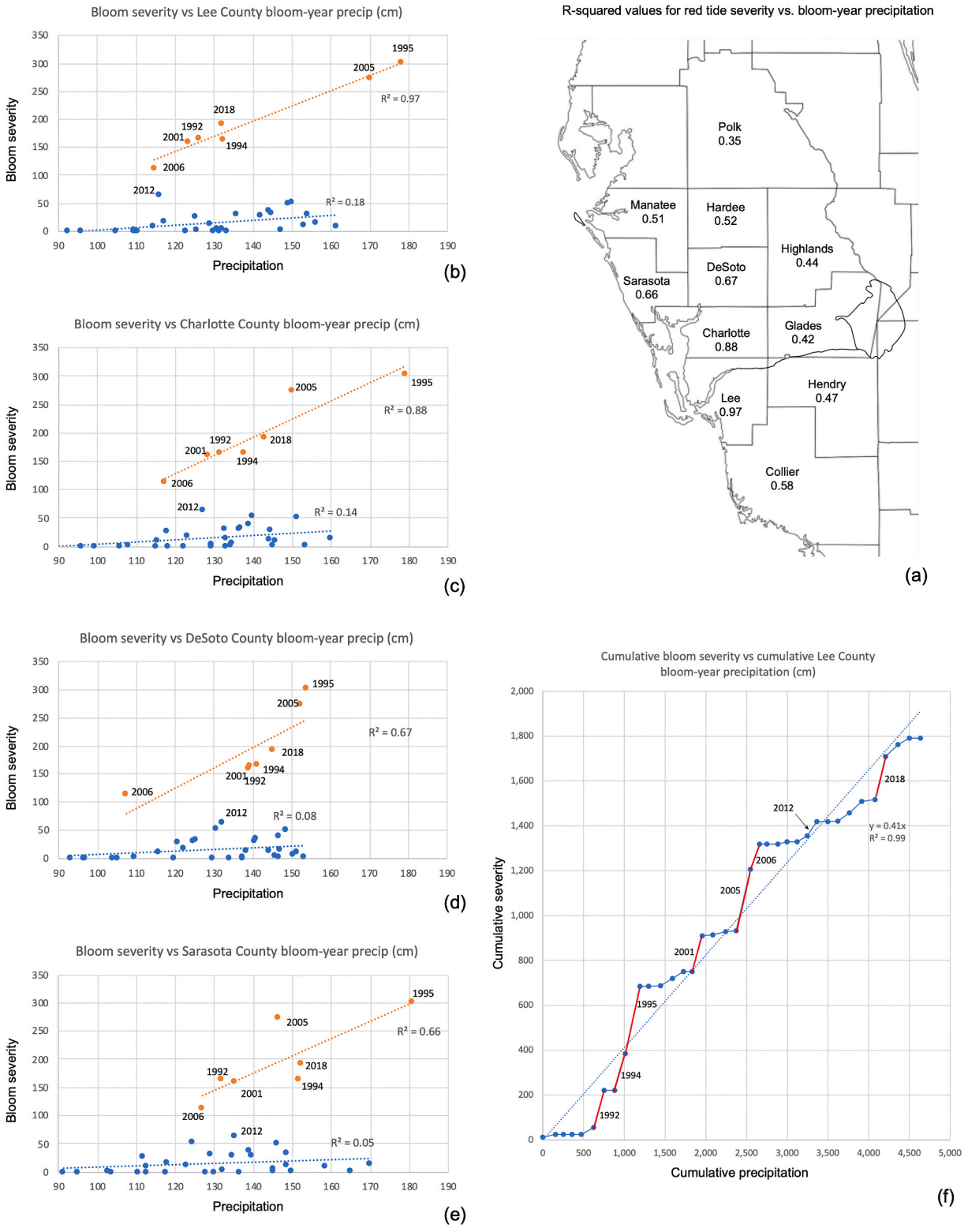

Fig. 7. (a) Values of R-squared for bloom severity (S_B) regressed against bloom-year precipitation in counties potentially contributing groundwater flows to the study region. (b–e) Bloom severities vs. bloom-year precipitation for Lee, Charlotte, DeSoto, and Sarasota counties. (f) Cumulative bloom severity vs. cumulative Lee County precipitation (red line segments mark red tides). (For interpretation of the references to colour in this figure legend, the reader is referred to the Web version of this article.)

3.3.1. History of bloom severities

The time series of *Kb* concentrations for each of the four study region sections, shown by Fig. 3a, have similar amplitudes and a high degree of synchrony, so bloom severities are based on the time series of *Kb* concentrations for the entire study region. Table 2 shows start date, start day-of-year, duration, maximum and average *Kb* concentrations, and severity (Eq. (2)) for each bloom. Data for '84–93 are less reliable than later data because sampling was initiated only after a bloom was detected and was limited to only a few locations. Those data were included in order to obtain a zero y-intercept in a subsequent regression calculation. Details are in the Supplemental Data File (S3 - Regression). The blooms marked as red tides were all described as such contemporaneously, while the other blooms were not.

Some researchers argue that red tides in the study region are more frequent and more severe than in the past because of an increase in nearshore nutrients caused by agricultural activities and urbanization, while others argue that this is an illusion caused by increased attention to the problem [20,154,155]. Table 2 shows no evidence of an increase in frequency or severity of *Kb* blooms over the study period. This is consistent with the relatively slight increase in the annual amount of fertilizer applied per unit of crop area in the U.S. during that time: most of the increase was between 1960 and about 1990 [85]. So, the past time period best suited for comparing past and present red tide frequencies and severities is prior to 1960, when fertilizer application was <25% of today's amount, but meaningful data on red tides that long ago are lacking.

3.3.2. Predicting the effect of precipitation on bloom severity

The DNRA hypothesis requires that change in bloom-year precipitation affects the severities of ordinary blooms and red tides differently. As long as DNRA is active, SGD-N reaching the sediment layer as NO_3^+ will be mostly converted to NH_4^+ and assimilated by the benthic sediment biomass. As a result, the amount of NO_3^+ that will break through into the water column will be small, so the *increase in severity of ordinary blooms with increasing bloom-year precipitation will be small* (and there will be no red tides). When DNRA ceases, there will be a release of accumulated N that will intensify a bloom to create a red tide and SGD-N reaching the benthic sediment layer will pass straight into the water column in an amount directly proportional to the SGD flow (thus directly proportional to the amount of precipitation), so the *increase in severity of red tides with increasing bloom-year precipitation will be large*. Calculated values for bloom severities and published data on precipitation will be used to test this prediction.

3.3.3. Testing the prediction

Fig. 7a shows R-squared values for linear regression of red tide bloom severity against bloom-year precipitation for all counties that can contribute groundwater flow to the coastal study region. The highest value is for Lee County (0.97, $p < 0.0001$), where offshore SGD from the LTA is likely to be a factor, but the lower values for Sarasota, DeSoto, and Charlotte counties are still highly significant (0.66–0.88, $p < 0.03$ to 0.002). While these three counties are unlikely to be a source of offshore SGD, precipitation-driven nearshore SGD from the water-table aquifer, along with surface runoff and stream flow, can contribute N to nearshore waters.

Fig. 7b–e shows plots of red tide and ordinary bloom severities against bloom-year precipitation for all four counties. As predicted, *the increase in red tide severity with increasing precipitation is large, while the increase in ordinary bloom severity is small*. Despite large differences in rainfall patterns between counties, the slopes of the regression lines (change in severity per unit change in precipitation amount) for red tide severities are quite similar. It was determined that precipitation in the years preceding a bloom has no influence on its severity.

Fig. 7f shows the relationship between cumulative bloom severity and Lee County cumulative precipitation from 1986 to 2021; details of the calculation are in Supplemental Data File S4 - Cumulative severity. The concentration of N in groundwater (or stream water and surface runoff) doesn't change very much, so the amount of precipitation is a rough proxy for the amount of N delivered to the bloom. Similarly, bloom size doesn't change very much, so bloom severity is a rough proxy for N uptake. This implies that, over a sufficiently long period of time, a plot of *cumulative* bloom severity (N uptake) vs. *cumulative* bloom-year precipitation (N delivered) should be a straight line, as confirmed by the figure (less reliable data on *Kb* concentrations for '86–93 were included in order to eliminate the y-intercept from the regression equation). Note that red tides do not occur when bloom severity is above the regression line (the '06 red tide is not an exception if it is treated as an extension of the '05 red tide).

A reasonable interpretation of the graph is that line segments with slopes lower than that of the regression line (blue) represent ordinary blooms that consumed *less than* the amount of N delivered by precipitation, the remainder having been *accumulated* by the benthic sediment biomass through DNRA, while line segments with slopes higher that the regression line (red) represent red tides that consumed *more than* the amount of N delivered, the remainder having been *released* from the benthic sediment biomass following cessation of DNRA. The N consumption attributable to red tides is about 75% of the total. If there was no N accumulation, the line segments would track along the regression line, as with the '12 bloom ($S_B = 64$), and there would be ordinary blooms every year, with the severity depending only on the amount of precipitation. It would require an extraordinary amount of precipitation in a single year to deliver enough N to create a red tide.

3.3.4. Other work on testing the hypothesis

The results reported here are the basis for ongoing fieldwork by the authors to characterize the offshore area where LTA SGD is likely to convey N to benthic sediment (Fig. 2a). This work includes determination of N concentrations at the top and bottom of the water column and determination of water column chlorophyll-a vertical concentration profiles along multiple E-W transects through the study area south and west of Sanibel Island. There are also plans for detection of SGD via installation of shallow monitoring wells in the seafloor that, if carried out, will give direct evidence of groundwater flow into benthic sediment.

4. Conclusions

Kb bloom severities are limited by the low availability of N during times when benthic DNRA is active because SGD-N is being accumulated in benthic biomass. Red tides occur when DNRA ceases due to exhaustion of sediment LOC and the accumulated N is released. When DNRA is inactive, increasing bloom-year precipitation increases transport of groundwater N into the water column. As a result, the severities of ordinary blooms are only slightly increased by increased bloom-year precipitation, while the severities of red tides are greatly increased.

Transport of groundwater N to offshore benthic sediment by SGD is consistent with the connection between local precipitation and monitoring-well groundwater levels, as well as with the location and hydrogeology of the LTA. This provides a firm foundation for further testing our hypothesis with observational data from the region where LTA SGD is likely.

That some, but not all, extreme precipitation events result in a red tide is predictable from our hypothesis. When DNRA is active, cumulative precipitation over several years transports SGD-N to benthic sediment, where it accumulates until the supply of benthic LOC is exhausted, stopping DNRA and releasing the N to support a red tide. No single precipitation event could do that, but a particularly heavy event might push the cumulative precipitation over the amount required to exhaust the LOC and appear to have "caused" a red tide.

A limitation in the hypothesis is its focus on offshore LTA SGD, so its extension to regions where offshore SGD is probably absent, but red tides are present, is not straightforward. Another limitation is its dependence on LOC availability, which is poorly understood and not easy to quantify.

The hypothesis suggests the possibility of reducing the severity of red tides, perhaps replacing them with ordinary blooms, by timely removal of marine life detritus so as to decrease the amount of LOC restored to the benthic sediment and the DNRA N-accumulation capacity of the benthic biomass. Timely removal of detritus would also decrease the availability of N in the water column, perhaps reducing the severity of a red tide in progress. In the absence of further validation, these potential benefits are highly speculative.

Author contribution statement

Bruce E. Kurtz & James E. Landmeyer: Conceived and designed the experiments; Analyzed and interpreted the data; Contributed reagents, materials, analysis tools or data; Wrote the paper.

James K. Culter: Conceived and designed the experiments; Performed the experiments; Analyzed and interpreted the data; Contributed reagents, materials, analysis tools or data.

Funding statement

This research did not receive any specific grant from funding agencies in the public, commercial, or not-for-profit sectors.

Data availability statement

Data included in article/supplementary material/referenced in article.

Declaration of competing interest

The authors declare that they have no known competing financial interests or personal relationships that could have appeared to influence the work reported in this paper.

Acknowledgements

The conception and initial development of this study would not have been possible without the guidance supplied by Ernie Estevez, Senior Scientist Emeritus, Mote Marine Laboratory. The comments and suggestions of an anonymous reviewer are also appreciated and have done much to improve the quality of this report. Any use of trade, firm, or product names is for descriptive purposes only and does not imply endorsement by the U.S. Government.

Appendix A. Supplementary data

Supplementary data to this article can be found online at https://doi.org/10.1016/j.heliyon.2023.e16046.

References

[1] R.H. Pierce, et al., Brevetoxin concentrations in marine aerosol: human exposure levels during a Karenia brevis harmful algal bloom, Bull. Environ. Contam. Toxicol. 70 (1) (2003) 161–165, https://doi.org/10.1007/s00128-002-0170-y.

[2] B. Kirkpatrick, et al., Literature review of Florida red tide: implications for human health effects, Harmful Algae 3 (2) (2004) 99–115, https://doi.org/10.1016/j.hal.2003.08.005.
[3] D.P. Gannon, et al., Effects of Karenia brevis harmful algal blooms on nearshore fish communities in southwest Florida, Mar. Ecol. Prog. Ser. 378 (2009) 171–186, https://doi.org/10.3354/meps07853.
[4] P. Hoagland, et al., The costs of respiratory illnesses arising from Florida gulf coast Karenia brevis blooms, Environ. Health Perspect. 117 (8) (2009) 1239–1243, https://doi.org/10.1289/ehp.0900645.
[5] B. Kirkpatrick, et al., Gastrointestinal emergency room admissions and Florida red tide blooms, Harmful Algae 9 (1) (2010) 82–86, https://doi.org/10.1016/j.hal.2009.08.005.
[6] L.E. Fleming, et al., Review of Florida red tide and human health effects, Harmful Algae 10 (2) (2011) 224–233, https://doi.org/10.1016/j.hal.2010.08.006.
[7] D.G. Baden, A.J. Bourdelais, H. Jacocks, S. Michelliza, J. Naar, Natural and derivative brevetoxins: historical background, multiplicity, and effects, Environ. Health Perspect. 113 (5) (2005) 621–625, https://doi.org/10.1289/ehp.7499.
[8] A.J. Bourdelais, H.M. Jacocks, J.L. Wright, P.M. Bigwarfe Jr., D.G. Baden, A new polyether ladder compound produced by the dinoflagellate Karenia brevis, J. Nat. Prod. 68 (1) (2005) 2–6, https://doi.org/10.1021/np049797o.
[9] D.R. Hardison, W.G. Sunda, R. Wayne Litaker, D. Shea, P.A. Tester, Nitrogen limitation increases brevetoxins in *Karenia brevis* (Dinophyceae): implications for bloom toxicity, J. Phycol. 48 (4) (2012) 844–858, https://doi.org/10.1111/j.1529-8817.2012.01186.x.
[10] K. Calabro, et al., Further insights into brevetoxin metabolism by de novo radiolabeling, Toxins 6 (6) (2014) 1785–1798, https://doi.org/10.3390/toxins6061785.
[11] S. L.Larkin, R. L.Degner, and C. M.Addams, "Final Report: Economic Effects of HABs on Coastal Communities and Shellfish Culture in Florida," U.S. Environmental Protection Agency, 2007, vol. EPA Grant Number: R831707.
[12] D.M. Anderson, et al., Harmful algal blooms and eutrophication: examining linkages from selected coastal regions of the United States, Harmful Algae 8 (1) (2008) 39–53, https://doi.org/10.1016/j.hal.2008.08.017.
[13] G.A. Vargo, A brief summary of the physiology and ecology of Karenia brevis Davis (G. Hansen and Moestrup comb. nov.) red tides on the West Florida Shelf and of hypotheses posed for their initiation, growth, maintenance, and termination, Harmful Algae 8 (4) (2009) 573–584, https://doi.org/10.1016/j.hal.2008.11.002.
[14] P.A. Tester, K.A. Steidinger, Gymnodinium breve red tide blooms: initiation, transport, and consequences of surface circulation, Limnol. Oceanogr. 42 (5) (1997) 1039–1051.
[15] G.A. Vargo, et al., Nutrient availability in support of Karenia brevis blooms on the central West Florida Shelf: what keeps Karenia blooming? Continent. Shelf Res. 28 (1) (2008) 73–98, https://doi.org/10.1016/j.csr.2007.04.008.
[16] K. Davidson, et al., Harmful algal blooms: how strong is the evidence that nutrient ratios and forms influence their occurrence? Estuar. Coast Shelf Sci. 115 (2012) 399–413, https://doi.org/10.1016/j.ecss.2012.09.019.
[17] Y. Liu, R.H. Weisberg, J.M. Lenes, L. Zheng, K. Hubbard, J.J. Walsh, Offshore forcing on the 'pressure point' of the West Florida Shelf: anomalous upwelling and its influence on harmful algal blooms, J. Geophys. Res. Oceans 121 (8) (2016) 5501–5515, https://doi.org/10.1002/2016jc011938.
[18] R.H. Weisberg, L. Zheng, Y. Liu, West Florida shelf upwelling: origins and pathways, J. Geophys. Res. Oceans 121 (2016) 5672–5681, 10.1002/.
[19] K.A. Steidinger, Basic Factors Influencing Red Tides, in: Proceedings of the First International Conference on Toxic Dinoflagellate Blooms, 1974.
[20] C.A. Heil, et al., Blooms of Karenia brevis (Davis) G. Hansen & Ø. Moestrup on the West Florida Shelf: nutrient sources and potential management strategies based on a multi-year regional study, Harmful Algae 38 (2014) 127–140, https://doi.org/10.1016/j.hal.2014.07.016.
[21] R.H. Weisberg, Y. Liu, C. Lembke, C. Hu, K. Hubbard, M. Garrett, The coastal ocean circulation influence on the 2018 west Florida shelf, J. Geophys. Res. Oceans (2019), https://doi.org/10.1029/2018jc014887.
[22] J.M. Lenes, B.A. Darrow, C. Cattrall, C. Heil, M. Callahan, Iron fertilization and the Trichodesmium response on the West Florida shelf, Limnol. Oceanogr. 46 (6) (2001) 1261–1277.
[23] J.J. Walsh, et al., Red tides in the Gulf of Mexico: where, when, and why? J. Geophys. Res. 111 (C11003) (2006) 1–46, https://doi.org/10.1029/2004JC002813.
[24] J.M. Lenes, et al., Saharan dust and phosphatic fidelity: a three-dimensional biogeochemical model of Trichodesmium as a nutrient source for red tides on the West Florida Shelf, Continent. Shelf Res. 28 (9) (2008) 1091–1115, https://doi.org/10.1016/j.csr.2008.02.009.
[25] J.M. Lenes, C.A. Heil, A historical analysis of the potential nutrient supply from the N2 fixing marine cyanobacterium Trichodesmium spp. to Karenia brevis blooms in the eastern Gulf of Mexico, J. Plankton Res. 32 (10) (2010) 1421–1431, https://doi.org/10.1093/plankt/fbq061.
[26] R.E. Sipler, et al., Trichodesmium-derived dissolved organic matter is a source of nitrogen capable of supporting the growth of toxic red tide Karenia brevis, Mar. Ecol. Prog. Ser. 483 (2013) 31–45, https://doi.org/10.3354/meps10258.
[27] L.B. Slobodkin, A possible initial condition for red tides on the coast of Florida, J. Mar. Res. IX (1) (1953) 148–155.
[28] J.H. Finucane, Distribution and Seasonal Occurrence of Gymnodinium Breve on the West Coast of Florida, 1954-57, vol. Special Scientific Report - Fisheries No. 487, U.S. Fish & Wildlife Service, 1964.
[29] C. Hu, F.E. Muller-Karger, P.W. Swarzenski, Hurricanes, submarine groundwater discharge, and Florida's red tides, Geophys. Res. Lett. 33 (11) (2006), https://doi.org/10.1029/2005gl025449.
[30] C.G. Smith, Submarine groundwater discharge along the West Florida Shelf: is groundwater an important nutrient source for Florida's red tides?, in: USGS - Sound Waves Monthly Newsletter USGS, 2009 vol. June/July 2009.
[31] C.G. Smith, P.W. Swarzenski, An investigation of submarine groundwater-borne nutrient fluxes to the west Florida shelf and recurrent harmful algal blooms, Limnol. Oceanogr. 57 (2) (2012) 471–485, https://doi.org/10.4319/lo.2012.57.2.0471.
[32] M. Taniguchi, W.C. Burnett, J.E. Cable, J.V. Turner, Investigation of submarine groundwater discharge, Hydrol. Process. 16 (11) (2002) 2115–2129, https://doi.org/10.1002/hyp.1145.
[33] W.C. Burnett, et al., Quantifying submarine groundwater discharge in the coastal zone via multiple methods, Sci. Total Environ. 367 (2–3) (2006) 498–543, https://doi.org/10.1016/j.scitotenv.2006.05.009.
[34] K.D. Kroeger, P.W. Swarzenski, W.J. Greenwood, C. Reich, Submarine groundwater discharge to Tampa Bay: nutrient fluxes and biogeochemistry of the coastal aquifer, Mar. Chem. 104 (1–2) (2007) 85–97, https://doi.org/10.1016/j.marchem.2006.10.012.
[35] J.B. Martin, J.E. Cable, C. Smith, M. Roy, J. Cherrier, Magnitudes of submarine groundwater discharge from marine and terrestrial sources: Indian River Lagoon, Florida, Water Resour. Res. 43 (5) (2007), https://doi.org/10.1029/2006wr005266.
[36] W.S. Moore, The effect of submarine groundwater discharge on the ocean, Ann. Rev. Mar. Sci 2 (2010) 59–88, https://doi.org/10.1146/annurev-marine-120308-081019.
[37] K.L. Knee, A. Paytan, Submarine groundwater discharge: a source of nutrients, metals, and pollutants to the coastal ocean, in: E. Wolanski, D. McLusky (Eds.), Treatise on Estuarine and Coastal Science, vol. 4, 2011, pp. 205–233.
[38] Q. Liu, M.A. Charette, P.B. Henderson, D.C. McCorkle, W. Martin, M. Dai, Effect of submarine groundwater discharge on the coastal ocean inorganic carbon cycle, Limnol. Oceanogr. 59 (5) (2014) 1529–1554, https://doi.org/10.4319/lo.2014.59.5.1529.
[39] V. Rodellas, J. Garcia-Orellana, P. Masque, M. Feldman, Y. Weinstein, Submarine groundwater discharge as a major source of nutrients to the Mediterranean Sea, Proc. Natl. Acad. Sci. U. S. A. 112 (13) (2015) 3926–3930, https://doi.org/10.1073/pnas.1419049112.
[40] M. Taniguchi, et al., Submarine groundwater discharge: updates on its measurement techniques, geophysical drivers, magnitudes, and effects, Front. Environ. Sci. 7 (2019), https://doi.org/10.3389/fenvs.2019.00141.
[41] E. Luijendijk, T. Gleeson, N. Moosdorf, Fresh groundwater discharge insignificant for the world's oceans but important for coastal ecosystems, Nat. Commun. 11 (1) (2020) 1260, https://doi.org/10.1038/s41467-020-15064-8.
[42] I.R. Santos, et al., Submarine groundwater discharge impacts on coastal nutrient biogeochemistry, Nat. Rev. Earth Environ. (2021), https://doi.org/10.1038/s43017-021-00152-0.

[43] D.A. Bronk, et al., Nitrogen uptake and regeneration (ammonium regeneration, nitrification and photoproduction) in waters of the West Florida Shelf prone to blooms of Karenia brevis, Harmful Algae 38 (2014) 50–62, https://doi.org/10.1016/j.hal.2014.04.007.
[44] B.G. Katz, J.K. Bohlke, Monthly Variability and Possible Sources of Nitrate in Ground Water beneath Mixed Agricultural Land Use, Suwannee and Lafayette Counties, Florida, USGS, Tallahassee, FL, 2000.
[45] N.M. Dubrovsky, et al., The quality of our nation's water— nutrients in the nation's streams and groundwater, 1992–2004, in: Circular 1350, USGS, Reston, Virginia, 2010. National Water-Quality Assessment Program.
[46] B.P. Koch, G. Kattner, M. Witt, U. Passow, Molecular insights into the microbial formation of marine dissolved organic matter: recalcitrant or labile? Biogeosciences 11 (15) (2014) 4173–4190, https://doi.org/10.5194/bg-11-4173-2014.
[47] D.E. LaRowe, et al., The fate of organic carbon in marine sediments - new insights from recent data and analysis, Earth Sci. Rev. 204 (2020), https://doi.org/10.1016/j.earscirev.2020.103146.
[48] C.Reich, "Investigation of Submarine Groundwater Discharge along the Tidal Reach of the Caloosahatchee River, Southwest Florida," USGS, Reston, VA, 2009, vol. Open-file report 2009-1273.
[49] L.A. Wedderburn, M.S. Knapp, D.P. Waltz, W.S. Burns, Hydrogeologic Reconnaissance of Lee County, Florida, South Florida Water Management Division, 1982.
[50] S.D. Weedman, F.L. Paillet, G.H. Means, T.M. Scott, Lithology and Geophysics of the Surficial Aquifer System in Western Collier County, Florida, vol. Open File Report 97-436, USGS, 1997.
[51] H. Klein, M.C. Schroeder, W.F. Lichter, Geology and Groundwater Resources of Glades and Hendry Counties, USGS, Florida, 1964.
[52] R.S. Reese, K.G. Cunningham, Hydrogeology of the Gray Limestone Aquifer in Southern Florida, USGS, 2000.
[53] D.H. Boggess, The Shallow Freshwater System of Sanibel Island, Lee County, Florida, with Emphasis on the Sources and Effects of Saline Water, USGS, Tallahassee, Florida, 1974.
[54] M.S. Knapp, W.S. Burns, T.S. Sharp, Preliminary Assessement of the Groundwater Resources of Western Collier County, Florida, South Florida Water Management Division, West Palm Beach, Florida, 1986.
[55] USGS-SAS, "United States Geological Survey - GROUND WATER ATLAS of the UNITED STATES Alabama, Florida, Georgia, South Carolina HA 730-G, Surficial Aquifer System." [Online]. Available: https://pubs.usgs.gov/ha/ha730/ch_g/.
[56] A.D. Duerr, G.M. Enos, Hydrogeology of the Intermediate Aquifer System and Upper Floridan Aquifer, Hardee and De Soto Counties, Florida, USGS, Tallahassee, Florida, 1991.
[57] G.L. Barr, Hydrogeology of the Surficial and Intermediate Aquifer Systems in Sarasota and Adjacent Counties, Florida, USGS, Tallahessee, Florida, 1996.
[58] USGS-IAS, "United States Geological Survey - GROUND WATER ATLAS of the UNITED STATES Alabama, Florida, Georgia, South Carolina HA 730-G , Intermediate Aquifer System." [Online]. Available: https://pubs.usgs.gov/ha/ha730/ch_g/.
[59] R.M. Wolansky, Hydrogeology of the Sarasota-Port Charlotte Area, Florida, USGS, Tallahassee, Florida, 1983.
[60] A.D. Duerr, R.M. Wolansky, Hydrology of the Surficial and Intermediate Aquifers of Central Sarasota County, Florida, USGS, Tallahassee, Florida, 1986.
[61] R.E. Glover, The pattern of fresh water flow in a coastal aquifer, J. Geophys. Res. 64 (4) (1959).
[62] H.H. Cooper, F.A. Kohout, H.R. Henry, R.E. Glover, Sea Water in Coastal Aquifers: Relation of Salt Water to Fresh Groundwater, 1964.
[63] M. Pool, J. Carrera, A correction factor to account for mixing in Ghyben-Herzberg and critical pumping rate approximations of seawater intrusion in coastal aquifers, Water Resour. Res. 47 (5) (2011), https://doi.org/10.1029/2010wr010256.
[64] L. Martínez-Pérez, et al., A multidisciplinary approach to characterizing coastal alluvial aquifers to improve understanding of seawater intrusion and submarine groundwater discharge, J. Hydrol. (2022), https://doi.org/10.1016/j.jhydrol.2022.127510.
[65] D. Adyasari, C. Hassenruck, D. Montiel, N. Dimova, Microbial community composition across a coastal hydrological system affected by submarine groundwater discharge (SGD), PLoS One 15 (6) (2020) e0235235, https://doi.org/10.1371/journal.pone.0235235.
[66] I.R. Santos, W.C. Burnett, T. Dittmar, I.G.N.A. Suryaputra, J. Chanton, Tidal pumping drives nutrient and dissolved organic matter dynamics in a Gulf of Mexico subterranean estuary, Geochem. Cosmochim. Acta 73 (5) (2009) 1325–1339, https://doi.org/10.1016/j.gca.2008.11.029.
[67] D.G. Capone, D.A. Bronk, M.R. Mulholland, E.J. Carpenter, Nitrogen in the Marine Environment, 2008.
[68] I. Koike, J. Sorensen, Nitrate reduction and denitrification in marine sediments, in: T.H. Blackburn, J. Sorensen (Eds.), Nitrogen Cycling in Coastal Marine Environments, 1988.
[69] G.T. Taylor, C. Gobler, S.A. Sanuudo-Wilhelmy, Speciation and concentrations of dissolved nitrogen as determinants of brown tide Aureococcus anophagefferens bloom initiation, Mar. Ecol. Prog. Ser. 312 (2006) 67–83.
[70] P.M. Glibert, et al., Phytoplankton communities from San Francisco Bay Delta respond differently to oxidized and reduced nitrogen substrates even under conditions that would otherwise suggest nitrogen sufficiency, Front. Mar. Sci. 1 (2014), https://doi.org/10.3389/fmars.2014.00017.
[71] P.M. Glibert, et al., Pluses and minuses of ammonium and nitrate uptake and assimilation by phytoplankton and implications for productivity and community composition, with emphasis on nitrogen-enriched conditions, Limnol. Oceanogr. 61 (1) (2016) 165–197, https://doi.org/10.1002/lno.10203.
[72] W.A. Wurtsbaugh, H.W. Paerl, W.K. Dodds, Nutrients, eutrophication and harmful algal blooms along the freshwater to marine continuum, WIREs Water 6 (5) (2019), https://doi.org/10.1002/wat2.1373.
[73] H. Sutcliffe, Appraisal of the Water Resources of Charlotte County, Florida, USGS, Tallahasee, Florida, 1973.
[74] R.K. Krulikas, G.L. Giese, Recharge to the Surficial Aquifer System in Lee and Hendry Counties, Florida, USGS, Tallahassee, Florida, 1995.
[75] E. Geddes, E. Richardson, A. Dodd, Hydrogeologic Unit Mapping Update for the Lower West Coast Water Supply Planning Area, South Florida Water Management Division, West Palm Beach, Florida, 2015.
[76] D.H. Boggess, T.H. O'Donnell, Deep Artesian Aquifers of Sanibel and Captiva Islands, Lee County, Florida, USGS, Tallahassee, Florida, 1982.
[77] H.J. McCoy, Groundwater Resources of Collier County, USGS, Florida, 1962.
[78] D.H. Boggess, F.A. Watkins, Surficial Aquifer System in Eastern Lee County, Florida, USGS, Tallahassee, Florida, 1986 vol. Water-ressources investigations report 85-4161.
[79] K.R. Smith, K.M. Adams, Groundwater Resource Assessment of Hendry County, South Florida Water Management Division, Florida, 1988.
[80] Missimer, Immokalee Area Study Stage II Technical Memorandum Groundwater Issues, CDM, 2002.
[81] P.K. Fairbank, S.M. Hohner, Mapping Recharge (Infiltration/leakage) throughout the South Florida Water Management District, South Florida Water Management Division, West Palm Beach, 1995 vol. Technical publication 95-02 (DRE 327).
[82] T. McKenzie, H. Dulai, P. Fuleky, Traditional and novel time-series approaches reveal submarine groundwater discharge dynamics under baseline and extreme event conditions, Sci. Rep. 11 (1) (Nov 19 2021), 22570, https://doi.org/10.1038/s41598-021-01920-0.
[83] P. Glibert, R. Maranger, D.J. Sobota, L. Bouwman, The Haber Bosch–harmful algal bloom (HB–HAB) link, Environ. Res. Lett. 9 (2014), 105001.
[84] P.M. Vitousek, et al., Human alteration of the global nitrogen cycle:sources and consequences, Ecol. Appl. 7 (3) (1997) 737–750.
[85] EPA. "Environmental Protection Agency, Fertilizer Applied for Agricultural Purposes. Retrieved from https://cfpub.epa.gov/roe/indicator.cfm?i=55." https://cfpub.epa.gov/roe/indicator.cfm?i=55 (accessed.
[86] R.E. Turner, et al., Paleo-indicators and water quality change in the Charlotte Harbor Estuary (Florida), Limnol. Oceanogr. 51 (1) (2006) 518–533, https://doi.org/10.4319/lo.2006.51.1_part_2.0518, part 2.
[87] C. Masclaux-Daubresse, F. Daniel-Vedele, J. Dechorgnat, F. Chardon, L. Gaufichon, A. Suzuki, Nitrogen uptake, assimilation and remobilization in plants: challenges for sustainable and productive agriculture, Ann. Bot. 105 (7) (2010) 1141–1157, https://doi.org/10.1093/aob/mcq028.
[88] R. Mylavarapu, W. Harris, G. Hochmuth, Agricultural Soils of Florida, U. of Florida, IFAS Extension, 2019.
[89] J.H. Viers, D. Liptzin, T.S. Rosenstock, V.B. Jensen, A.D. Hollander, Nitrogen sources and loading to groundwater, in: Addressing Nitrate in California's Drinking Water, University of California, Davis, 2012.
[90] J.K. Böhlke, R.L. Smith, D.N. Miller, Ammonium transport and reaction in contaminated groundwater: application of isotope tracers and isotope fractionation studies, Water Resour. Res. 42 (5) (2006), https://doi.org/10.1029/2005wr004349.

[91] Y. Umezawa, et al., Sources of nitrate and ammonium contamination in groundwater under developing Asian megacities, Sci. Total Environ. 404 (2–3) (2008) 361–376, https://doi.org/10.1016/j.scitotenv.2008.04.021.
[92] A.F. Rusydi, et al., Potential sources of ammonium-nitrogen in the coastal groundwater determined from a combined analysis of nitrogen isotope, biological and geological parameters, and land use, Water 13 (1) (2020), https://doi.org/10.3390/w13010025.
[93] B.T. Nolan, K.J. Hitt, B.C. Ruddy, Probability of nitrate contamination of recently recharged ground waters in the conterminous United States, Environ. Sci. Technol. 36 (10) (2002) 2138–2145.
[94] N.M. Dubrovsky, Nutrients in the Nation's Streams and Groundwater, 1992–2004 – Implications for Human Health, Aquatic Life, and Managing Nutrients in Our Water Resources, vol. Nutrient briefing sheet, USGS, 2010.
[95] M. Sebilo, B. Mayer, B. Nicolardot, G. Pinay, A. Mariotti, Long-term fate of nitrate fertilizer in agricultural soils, Proc. Natl. Acad. Sci. U. S. A. 110 (45) (Nov 5 2013) 18185–18189, https://doi.org/10.1073/pnas.1305372110.
[96] K.J. Van Meter, N.B. Basu, J.J. Veenstra, C.L. Burras, The nitrogen legacy: emerging evidence of nitrogen accumulation in anthropogenic landscapes, Environ. Res. Lett. 11 (3) (2016), https://doi.org/10.1088/1748-9326/11/3/035014.
[97] K.J. Van Meter, P. Van Cappellen, N.B. Basu, Legacy nitrogen may prevent achievement of water quality goals in the Gulf of Mexico, Science 360 (6387) (2018) 427–430, https://doi.org/10.1126/science.aar4462.
[98] USGS-NWIS. United States Geological Survey – National Water Information System: Mapper. Retrieved from https://maps.waterdata.usgs.gov/mapper/index.html. Accessed February 2022 [Online] Available: https://maps.waterdata.usgs.gov/mapper/index.html.
[99] DBHYDRO. South Florida Water Management District, DBHYDRO (Environmental Data). Retrieved from https://www.sfwmd.gov/science-data/dbhydro . Accessed February 2022. [Online] Available: http://my.sfwmd.gov/dbhydroplsql/show_dbkey_info.main_menu.
[100] NOAA-NCEI. NOAA – National Centers for Environmental Information, retrieved from https://www.ncei.noaa.gov/access/monitoring/climate-at-a-glance/. Accessed September 2022. [Online] Available: https://www.ncdc.noaa.gov/cag/.
[101] R.P. Stumpf, et al., Quantifying Karenia brevis bloom severity and respiratory irritation impact along the shoreline of Southwest Florida, PLoS One 17 (1) (2022) e0260755, https://doi.org/10.1371/journal.pone.0260755.
[102] D. Chagaris, D. Sinnickson, An Index of Red Tide Mortality on Red Grouper in the Eastern Gulf of Mexico, SEDAR61-WP-06, 2018, p. 16.
[103] W. Gyhben, Notes on the probable results of the proposed well drilling near Amsterdam, 1888-89, The Hague, Ing. Tijdschr. (1889) 8–22.
[104] A. Herzberg, The water supply on parts of the North Sea coast, J. Gasbeleucht. Wasserversorg 44 (1901), pp. 815–819, 842-844.
[105] M. Diego-Feliu, V. Rodellas, A. Alorda-Kleinglass, M. Saaltink, A. Folch, J. Garcia-Orellana, Extreme precipitation events induce high fluxes of groundwater and associated nutrients to coastal ocean, vol. Preprint, Hydrol. Earth Syst. Sci. (2022), https://doi.org/10.5194/hess-2021-594.
[106] D. Lyons-Morancy, "Evapotranspiration," (South Florida Water Management District).
[107] Atkins, Collier County Watershed Management Plan, Collier County, Florida, Atkins, Tampa, Florida, 2011.
[108] Collier County, Collier County Reclaimed Water Factsheet, 2018.
[109] USGS, "United States Geological Survey - Nutrients in the Nation's Streams and Groundwater: National Findings and Implications.".
[110] Y. Weinstein, Y. Yechieli, Y. Shalem, W.C. Burnett, P.W. Swarzenski, B. Herut, What is the role of fresh groundwater and recirculated seawater in conveying nutrients to the coastal ocean? Environ. Sci. Technol. 45 (12) (2011) 5195–5200, https://doi.org/10.1021/es104394r.
[111] W.R. Henson, L. Huang, W.D. Graham, A. Ogram, Nitrate reduction mechanisms and rates in an unconfined eogenetic karst aquifer in two sites with different redox potential, J. Geophys. Res.: Biogeosci. 122 (5) (2017) 1062–1077, https://doi.org/10.1002/2016jg003463.
[112] T.B. Kelly, et al., Lateral advection supports nitrogen export in the oligotrophic open-ocean Gulf of Mexico, Nat. Commun. 12 (1) (2021) 3325, https://doi.org/10.1038/s41467-021-23678-9.
[113] S. Uye, N. Iwamoto, T. Ueda, H. Tamaki, K. Nakahira, Geographical variations in the trophic structure of the plankton community along a eutrophic ±mesotrophic± oligotrophic transect, Fish. Oceanogr. 8 (3) (1999) 227–237.
[114] G. Basterretxea, et al., Cross-shore environmental gradients in the western Mediterranean coast and their influence on nearshore phytoplankton communities, Front. Mar. Sci. 5 (2018), https://doi.org/10.3389/fmars.2018.00078.
[115] J. Kubanek, M.K. Hicks, J. Naar, T.A. Veillareal, Does the red tide dinoflagellate Karenia brevis use allelopathy to outcompete other phytoplankton? Limnol. Oceanogr. 50 (3) (2005) 883–895.
[116] E.K. Prince, T.L. Myers, J. Kubanek, Effects of harmful algal blooms on competitors: allelopathic mechanisms of the red tide dinoflagellate Karenia brevis, Limnol. Oceanogr. 53 (2) (2008) 531–541.
[117] K.L. Poulson, R.D. Sieg, E.K. Prince, J. Kubanek, Allelopathic compounds of a red tide dinoflagellate have species-specific and context-dependent impacts on phytoplankton, Mar. Ecol. Prog. Ser. 416 (2010) 69–78, https://doi.org/10.3354/meps08788.
[118] K. Poulson-Ellestad, E. McMillan, J.P. Montoya, J. Kubanek, Are offshore phytoplankton susceptible to Karenia brevis allelopathy? J. Plankton Res. 36 (5) (2014) 1344–1356, https://doi.org/10.1093/plankt/fbu064.
[119] K.L. Poulson-Ellestad, et al., Metabolomics and proteomics reveal impacts of chemically mediated competition on marine plankton, Proc. Natl. Acad. Sci. U. S. A. 111 (24) (Jun 17 2014) 9009–9014, https://doi.org/10.1073/pnas.1402130111.
[120] R.X. Poulin, S. Hogan, K.L. Poulson-Ellestad, E. Brown, F.M. Fernandez, J. Kubanek, Karenia brevis allelopathy compromises the lipidome, membrane integrity, and photosynthesis of competitors, Sci. Rep. 8 (1) (Jun 22 2018) 9572, https://doi.org/10.1038/s41598-018-27845-9.
[121] K. Salonen, M. Rosenberg, Advantages from diel vertical migration can explain the dominance of Gonyostomum semen (Raphidophyceae) in a small, steeply-stratified humic lake, J. Plankton Res. 22 (10) (2000) 1841–1853.
[122] J. Kerfoot, G. Kirkpatrick, S.E. Lohrenz, K. Mahoney, M. Moline, O.M. Schofield, Vertical migration of a K. brevis bloom: implications for remote sensing of HABs, in: Presented at the Proceedings of the Xth International Conference on Harmful Algae, October 2002, St. Petersburg, Florida, 2003. Contribution No. 681.
[123] O. Schofield, et al., Vertical migration of the toxic dinoflagellate Karenia brevis and the impact on ocean optical properties, J Geophys Res Oceans 111 (2006), https://doi.org/10.1029/2005jc003115. C6.
[124] B.A. Schaeffer, D. Kamykowski, G. Sinclair, L. McKay, E.J. Milligan, Diel vertical migration thresholds of Karenia brevis (Dinophyceae), Harmful Algae 8 (5) (2009) 692–698, https://doi.org/10.1016/j.hal.2009.01.002.
[125] F.M. Van Dolah, et al., The Florida red tide dinoflagellate Karenia brevis: new insights into cellular and molecular processes underlying bloom dynamics, Harmful Algae 8 (4) (2009) 562–572, https://doi.org/10.1016/j.hal.2008.11.004.
[126] C.A. Heil, et al., Influence of daylight surface aggregation behavior on nutrient cycling during a Karenia brevis (Davis) G. Hansen & Ø. Moestrup bloom: migration to the surface as a nutrient acquisition strategy, Harmful Algae 38 (2014) 86–94, https://doi.org/10.1016/j.hal.2014.06.001.
[127] O. Einsle, A. Messerschmidt, R. Huber, P.M. Kroneck, F. Neese, Mechanism of the six-electron reduction of nitrite to ammonia by cytochrome c nitrite reductase, J. Am. Chem. Soc. 124 (39) (2002) 11737–11745, https://doi.org/10.1021/ja0206487.
[128] J.A. Cole, C.M. Brown, Nitrite reduction to ammonia by fermentative bacteria: a short circuit in the biological nitrogen cycle, FEMS (Fed. Eur. Microbiol. Soc.) Microbiol. Lett. 7 (1980) 65–72.
[129] T.O. Strohm, B. Griffin, W.G. Zumft, B. Schink, Growth yields in bacterial denitrification and nitrate ammonification, Appl. Environ. Microbiol. 73 (5) (Mar 2007) 1420–1424, https://doi.org/10.1128/AEM.02508-06.
[130] A.J. Kessler, K.L. Roberts, A. Bissett, P.L.M. Cook, Biogeochemical controls on the relative importance of denitrification and dissimilatory nitrate reduction to ammonium in estuaries, Global Biogeochem. Cycles 32 (7) (2018) 1045–1057, https://doi.org/10.1029/2018gb005908.
[131] H.K. Carlson, et al., Selective carbon sources influence the end products of microbial nitrate respiration, ISME J. 14 (8) (2020) 2034–2045, https://doi.org/10.1038/s41396-020-0666-7.
[132] A. Giblin, C. Tobias, B. Song, N. Weston, G. Banta, V. Rivera-Monroy, The importance of dissimilatory nitrate reduction to ammonium (DNRA) in the nitrogen cycle of coastal ecosystems, Oceanography 26 (3) (2013) 124–131, https://doi.org/10.5670/oceanog.2013.54.

[133] G.D. Song, S.M. Liu, H. Marchant, M.M.M. Kuypers, G. Lavik, Anaerobic ammonium oxidation, denitrification and dissimilatory nitrate reduction to ammonium in the East China Sea sediment, Biogeosci. Discuss. 10 (2013) 4671–4710, https://doi.org/10.5194/bgd-10-4671-2013.
[134] H.K. Marchant, G. Lavik, M. Holtappels, M.M. Kuypers, The fate of nitrate in intertidal permeable sediments, PLoS One 9 (8) (2014) e104517, https://doi.org/10.1371/journal.pone.0104517.
[135] E.M. van den Berg, M.P. Elisario, J.G. Kuenen, R. Kleerebezem, M.C.M. van Loosdrecht, Fermentative bacteria influence the competition between denitrifiers and DNRA bacteria, Front. Microbiol. 8 (2017) 1684, https://doi.org/10.3389/fmicb.2017.01684.
[136] S. An, W.S. Gardner, Dissimilatory nitrate reduction to ammonium (DNRA) as a nitrogen link, versus denitrification as a sink in a shallow estuary (Laguna Madre/Baffin Bay, Texas), Mar. Ecol. Prog. Ser. 237 (2002) 41–50.
[137] B. Song, J.A. Lisa, C.R. Tobias, Linking DNRA community structure and activity in a shallow lagoonal estuarine system, Front. Microbiol. 5 (2014) 460, https://doi.org/10.3389/fmicb.2014.00460.
[138] R.J. Bernard, B. Mortazavi, A.A. Kleinhuizen, Dissimilatory nitrate reduction to ammonium (DNRA) seasonally dominates NO3- reduction pathways in an anthropogenically impacted sub-tropical coastal lagoon, Biogeochemistry 125 (1) (2015) 47–64, https://doi.org/10.1007/s10533-015-0111-6.
[139] K.R. Salk, D.V. Erler, B.D. Eyre, N. Carlson-Perret, N.E. Ostrom, Unexpectedly high degree of anammox and DNRA in seagrass sediments: description and application of a revised isotope pairing technique, Geochem. Cosmochim. Acta 211 (2017) 64–78, https://doi.org/10.1016/j.gca.2017.05.012.
[140] S. Nayar, M.G.K. Loo, J.E. Tanner, A.R. Longmore, G.P. Jenkins, Nitrogen acquisition and resource allocation strategies in temperate seagrass Zostera nigricaulis: uptake, assimilation and translocation processes, Sci. Rep. 8 (1) (2018), 17151, https://doi.org/10.1038/s41598-018-35549-3.
[141] M.M. Jensen, B. Thamdrup, T. Dalsgaard, Effects of specific inhibitors on anammox and denitrification in marine sediments, Appl. Environ. Microbiol. 73 (10) (May 2007) 3151–3158, https://doi.org/10.1128/AEM.01898-06.
[142] H. Dang, et al., Environmental factors shape sediment anammox bacterial communities in hypernutrified Jiaozhou Bay, China, Appl. Environ. Microbiol. 76 (21) (Nov 2010) 7036–7047, https://doi.org/10.1128/AEM.01264-10.
[143] C. Schleper, G.W. Nicol, Ammonia-oxidising archaea–physiology, ecology and evolution, Adv. Microb. Physiol. 57 (2010) 1–41, https://doi.org/10.1016/B978-0-12-381045-8.00001-1.
[144] D.A. Stahl, J.R. de la Torre, Physiology and diversity of ammonia-oxidizing archaea, Annu. Rev. Microbiol. 66 (2012) 83–101, https://doi.org/10.1146/annurev-micro-092611-150128.
[145] K.D. Kits, et al., Kinetic analysis of a complete nitrifier reveals an oligotrophic lifestyle, Nature 549 (7671) (2017) 269–272, https://doi.org/10.1038/nature23679.
[146] a. Brune, P. Frenzel, C. H, Life at the oxic-anoxic interface: microbial activities and adaptations, FEMS Microbiol. Rev. 24 (2000) 691–710.
[147] R.J. Lukatelich, A.J. McComb, Distribution and abundance of benthic microalgae in a shallow southwestern Australian estuarine system, Mar. Ecol.: Prog. Ser. 27 (1986) 287–297.
[148] J.L. Pinckney, S. Zaunbrecher, S. Lang, A. Wilson, A. Knapp, Seasonality of benthic microalgal community abundance in shallow shelf waters, Continent. Shelf Res. 244 (2022), https://doi.org/10.1016/j.csr.2022.104797.
[149] J.L. Pinkney, A mini-review of the contribution of benthic microalgae to the ecology of the continental shelf in the South atlantic Bight, Estuar. Coast 41 (7) (2018) 2070–2078, https://doi.org/10.1007/s12237-018-0401-z.
[150] A. Kamp, D. de Beer, J.L. Nitsch, G. Lavik, P. Stief, Diatoms respire nitrate to survive dark and anoxic conditions, Proc. Natl. Acad. Sci. U. S. A. 108 (14) (Apr 5 2011) 5649–5654, https://doi.org/10.1073/pnas.1015744108.
[151] A. Kamp, S. Hogslund, N. Risgaard-Petersen, P. Stief, Nitrate storage and dissimilatory nitrate reduction by eukaryotic microbes, Front. Microbiol. 6 (2015) 1492, https://doi.org/10.3389/fmicb.2015.01492.
[152] B.D. Eyre, A.J.P. Ferguson, Benthic metabolism and nitrogen cycling in a subtropical east Australian estuary (Brunswick): temporal variability and controlling factors, Limnol. Oceanogr. 50 (2005) 81–96.
[153] K. Dähnke, A. Moneta, B. Veuger, K. Soetaert, J.J. Middelburg, Balance of assimilative and dissimilative nitrogen processes in a diatom-rich tidal flat sediment, Biogeosciences 9 (10) (2012) 4059–4070, https://doi.org/10.5194/bg-9-4059-2012.
[154] L.E. Brand, A. Compton, Long-term increase in Karenia brevis abundance along the southwest Florida coast, Harmful Algae 6 (2) (2007) 232–252, https://doi.org/10.1016/j.hal.2006.08.005.
[155] C. Hu, R. Luerssen, F.E. Muller-Karger, K.L. Carder, C.A. Heil, On the remote monitoring of Karenia brevis blooms of the west Florida shelf, Continent. Shelf Res. 28 (1) (2008) 159–176, https://doi.org/10.1016/j.csr.2007.04.014.